

Correlation networks: Interdisciplinary approaches beyond thresholding

Naoki Masuda^{1,2}, Zachary M. Boyd³, Diego Garlaschelli^{4,5}, and Peter J. Mucha⁶

¹Department of Mathematics, State University of New York at Buffalo

²Institute for Artificial Intelligence and Data Science, State University of New York at Buffalo

³Department of Mathematics, Brigham Young University

⁴Lorentz Institute for Theoretical Physics, Leiden University, The Netherlands

⁵IMT School of Advanced Studies, Lucca, Italy

⁶Department of Mathematics, Dartmouth College

Abstract

Many empirical networks originate from correlational data, arising in domains as diverse as psychology, neuroscience, genomics, microbiology, finance, and climate science. Specialized algorithms and theory have been developed in different application domains for working with such networks, as well as in statistics, network science, and computer science, often with limited communication between practitioners in different fields. This leaves significant room for cross-pollination across disciplines. A central challenge is that it is not always clear how to best transform correlation matrix data into networks for the application at hand, and probably the most widespread method, i.e., thresholding on the correlation value to create either unweighted or weighted networks, suffers from multiple problems. In this article, we review various methods of constructing and analyzing correlation networks, ranging from thresholding and its improvements to weighted networks, regularization, dynamic correlation networks, threshold-free approaches, and more. Finally, we propose and discuss a variety of key open questions currently confronting this field.

1 Introduction

Correlation matrices capture pairwise similarity of multiple, often temporally evolving signals, and are used to describe system interactions in various diverse disciplines of science and society, from financial economics to psychology, bioinformatics, neuroscience, and climate science, to name a few. Correlation analysis is often a first step in trying to understand complex systems data [1]. Existing methods for analyzing correlation matrix data are abundant. Very well established methods include principal component analysis (PCA) [2] and factor analysis (FA) [3,4], which can yield a small number of interpretable components from correlation matrices, such as a global market trend when applied to stock market data, or spatio-temporal patterns of air pressure when applied to atmospheric data. Another major method for analyzing correlation matrix data is the Markowitz's portfolio theory in mathematical finance, which aims to minimize the variance of financial returns while keeping the expected return above a given threshold [5,6]. In a related vein, random matrix theory has been a key theoretical tool for analyzing economic and other correlation matrix data for a couple of decades [6]. Various new methods for analyzing correlation matrix data have also been proposed. Examples include detrended cross-correlation analysis [7–9], correlation dependency, defined as the difference between the partial correlation coefficient and the Pearson correlation coefficient given three nodes [10,11], determination of optimal paths between distant locations in correlation matrix data [12], early warning signals for anticipating abrupt changes in multidimensional dynamical systems including the case of networked systems [13–15], and energy landscape analysis for multivariate time series data particularly employed in neuroscience [16,17].

The last two decades have also seen successful applications of tools from network science and graph theory to correlational data. A correlation matrix can be mapped onto a network, which we refer to here as a *correlation network*, where nodes represent elements and edges are informed by the strength of the correlation between pairs of elements. Correlation network analysis generally intends to extract useful information from data, such as the patterns of interactions among nodes or a ranking of nodes. An ideal correlation network analysis appropriately adapts concepts and methods developed in network science to the case of correlation networks, generating knowledge that standard methods for correlation matrices (such as PCA) do not produce. Although correlation does not necessarily reflect a physical connection or direct interaction between two nodes, correlation matrices are conventionally used as a relatively inexpensive substitute of such direct connections, whose data are often less available than correlation

matrix data. Correlation networks are also useful for visualization [18]. Correlation network analysis has been used in various research disciplines, typically not much behind wherever correlation matrix analysis is used, as we will review in section 2. In our survey here, we focus on correlation networks, with an emphasis on identifying different methods used to transform correlation matrices into correlation networks.

The validity of correlation network analysis remains an outstanding question, especially because the decisions about how to best construct network representations from correlation matrices is far from straightforward. One of the simplest methods is to threshold on the correlation value measured for each pair of nodes (see section 3.2). However, while such a simple thresholding is widely used, it introduces various problems. These problems have led to proposals of alternative methods for generating correlation networks, which we will cover in sections 3.3–3.6.

Before proceeding, we raise some important clarifications. First, correlation networks as we consider here are different from network architectures that exploit correlation in data. For example, the Progressive Spatio-Temporal Correlation Network (PSCC-net) is an algorithm to detect and localize manipulations in the input image data by taking advantage of spatial correlation structure in images [19]. The superpixel group-correlation network (SGCN) [20] and the deep correlation network (DCNet) [21] are encoder-decoder and deep-learning network architectures, respectively, for salient object detection in images. These “networks” are in the sense of neural network architecture in artificial intelligence and machine learning, whereas here we consider “networks” to denote graphs in network science.

Second, we focus on correlation networks based on the Pearson correlation coefficient or its close variants such as the partial correlation coefficient. In fact, there are numerous other definitions for quantifying the similarity between data obtained from node pairs [22–28]. Examples include similarity networks whose edges are determined using the rank correlation coefficient [29,30], the mutual information [31–33], and partial mutual information [34,35]. However, a majority of concepts and techniques explained in our main technical section, section 3, such as the detrimental effect of thresholding and dichotomizing the edge weight, use of weighted networks, graphical lasso, and importance of null model, also hold true when one constructs correlation networks using these or other alternative methods.

Third, we do not discuss causal inference in the present paper. The inherently symmetric nature of correlation matrices or general similarity matrices mean that these matrices or networks in principle do not inform us of causality or directionality between nodes. If the original data upon which one calculates correlation matrices and networks are multivariate time series, a plethora of methods are available for inferring causality between nodes and associated directed networks. For these techniques, see, e.g., [18, 28, 36, 37]. In a related vein, we do not discuss time-lagged correlation in this paper, since these are also asymmetric in general, although many of the same considerations we raise here also apply to lagged correlations.

2 Application areas

Correlation network analysis is common in many research fields. In this section, we survey typical correlation networks and their analysis in representative research fields.

2.1 Psychological networks

There are various multivariate psychological data, from which one can construct networks [18, 38]. For example, in personality research, researchers construct personality networks in which each node can be a personal trait or goal such as being organized, being lazy, and wanting to stay safe. Edges between a pair of nodes typically represent a type of conditional association between the two nodes. Samples are frequently participants in the research responding to various questionnaires on a numeric scale (e.g., 5-point scale ranging from 1: strongly disagree to 5: strongly agree) corresponding to nodes. From a cross-sectional data set, one can calculate (conditional) correlation between pairs of nodes. Researchers are also increasingly combining surveys with alternative data collection modalities, for example, sensor data for daily movement or neural markers of stress [39, 40]

Another major type of psychological network is symptom networks employed in mental health research. Symptoms of a psychological, including psychopathological, condition, such as major depression and schizophrenia, are interrelated. Furthermore, causality between symptoms such as fatigue, headaches, concentration problems, and insomnia, and a psychopathological disorder, is often unclear. It has been suggested that a disorder does not originate from a single root cause, which motivates the study of symptom networks [18, 41–43]. Nodes in a symptom network are symptoms, and one can use association between pairs of symptoms calculated from the participants’ responses to define edges. Analysis of symptom networks may help us to predict how an individual develops psychopathology in the future, understand comorbidity as strong connection between symptoms of two mental disorders, and propose central nodes as possible targets of intervention [43]. Health-promoting behaviors can also be treated as nodes in these networks to suggest key behavioral intervention points [44].

Panel data, i.e., longitudinal measurements of variables from samples, are increasingly common for network approaches [18]. In this case, one obtains correlation networks at multiple time points. Then, one can construct time-varying correlation networks (see section 3.7) or within-person correlation networks [45] that reflect temporal symptom patterns and ideally expose individual differences and possible causal pathways in mental health patterns related to disorders [46, 47]. However, the validity of psychological network approach should be further studied. Research has shown that symptom networks have poor reproducibility across samples, likely due to measurement error in assessing symptoms among other reasons [42, 48].

2.2 Brain networks

Various notions of brain connectivity have been essential to better understanding different neural functions. Studies of such brain networks constitute a major part of a research field that is often referred to as *network neuroscience* [49, 50]. (See also the related material about network representations in [51].) Multivariate time series of neuronal signals recorded from the brain are a major source of data used in network neuroscience research. Such data may be recorded in a resting state or when participants are performing some task. Functional networks or functional connectivity refer to correlation-based networks constructed from multivariate neuronal time series data, obtained through, e.g., neuroimaging or electroencephalography, where the term “functional” in this setting effectively means correlational. In the case of multivariate time series data, there are various other methods to infer directed brain networks, which is referred to as effective connectivity, but we do not cover directed networks in this article. Brain networks based on anatomical connectivity between brain regions are referred to as structural networks. Functional connectivity, or an correlation-based edge between two nodes in the brain does not imply the presence of an edge between the same pair of nodes in the structural network. A typical node in the functional and structural brain networks is either a voxel (i.e., cube of side length of, e.g., 1 mm) or a spherical region of interest (ROI), which is a sphere in the brain. See [25, 27, 49, 52] for review of brain networks, including functional networks.

The most typical functional neuronal networks come from neuroimaging data, in particular functional magnetic resonance imaging (fMRI) data, which are measured using blood-oxygenation-level-dependent (BOLD) imaging techniques [53]. Functional connectivity between voxels or between spherical ROIs, or other types of nodes, is calculated by a correlation between fMRI time signals at the two nodes after one has bandpassed the fMRI time series at each node to remove artifacts, with a frequency band of, e.g., 0.01-0.1 Hz. Functional MRI improves on electroencephalogram (EEG) and magnetoencephalography (MEG) in spatial resolution at the expense of temporal resolution, but functional EEG and MEG networks are not uncommon. We also note that EEG and MEG signals are oscillatory, so one has to calculate the functional connectivity between each pair of nodes using methods that are aware of the oscillatory nature of the signal, such as using phase lag index or amplitude envelope correlation [54] rather than conventional correlation coefficients or mutual information.

Structural covariance networks are another type of correlation brain network where the edges are defined as the correlation/covariance of the corrected gray matter volume or cortical thickness between brain regions i and j , where the samples are participants [55, 56]. Morphometric similarity networks are a variant of structural covariance networks. In morphometric similarity networks, one uses various morphometric variables, not just a single one such as cortical thickness, for each node (i.e., ROI) [57]. One calculates the correlation between two nodes by regarding each morphometric variable as a sample. Therefore, differently from structural covariance networks based on cortical thickness, one can calculate a correlation network for each individual.

In neuroreceptor similarity networks, an edge between two nodes, or ROIs, is the correlation in terms of receptor density [58]. Specifically, one first calculates a vector of neurotransmitter density for each ROI, with each entry of the vector corresponding to one type of receptor. Then, one computes the correlation between each pair of ROIs, called receptor similarity.

2.3 Gene co-expression networks

Genes do not work in isolation. Gene co-expression networks have been useful for figuring out webs of interaction among genes using network analysis methods [28, 59–66]. They are a type of data in a subfield of network science often referred to as *network biology* or *network medicine*. Gene co-expression networks are correlation networks in the generalized sense considered here, including the case of other measures of similarity. A typical measurement is the amount of gene expression for different genes and samples, where a sample most commonly corresponds to a human or animal individual. If one measures the expression of various genes for the same set of samples, we can calculate the co-expression between each pair of genes by calculating the sample correlation, yielding a correlation matrix. Depending on the questions being asked in the study, it may be important to calculate the underlying correlations with different factors to account for the effects of heterogeneous gene frequencies [67, 68]. It is common

to transform a correlation matrix into a network and then apply various network analysis methods, for example community detection with the aim of estimating the group of genes that are associated with the same phenotype¹ such as a disease. In this manner, correlation network analysis has been a useful tool for gene screening, which can lead to identification of biomarkers and therapeutic targets. In addition to community detection, identifying hub genes in co-expression networks helps finding key genes, for example, for cancer [69].

Different ways of defining co-expression matrices and networks from gene expression data include tissue-to-tissue co-expression (TTC) networks [70] (also see [71, 72]). A TTC network proposed in [70] is a bipartite network, and its node is a gene-tissue pair. An edge between two nodes, denoted by $(\tilde{g}_i, \tilde{t}_i)$ and $(\tilde{g}_j, \tilde{t}_j)$, where \tilde{g}_i and \tilde{g}_j are genes, and \tilde{t}_i and \tilde{t}_j are tissues, represents the sample correlation as in conventional co-expression networks. However, by definition, the correlation is calculated only between node pairs belonging to different tissues, i.e., only for $\tilde{t}_i \neq \tilde{t}_j$. Therefore, TTC networks characterize co-expression of genes across different tissues.

Co-expression of genes i and j implies that i and j are both expressed at a high level in some samples (usually individuals) and both expressed at a low level in other individuals. Co-expressed genes tend to be involved in common biological functions. There are in fact multiple biophysical and non-biophysical reasons for gene co-expression [63]. For example, a transcription factor, a protein that binds to DNA, may regulate different genes i and j that are physically close on a chromosome. If this is the case, differential levels of regulation by the transcription factor across individuals can create co-expression of i and j . Another mechanism of co-expression is that the expression of genes i and j , which may be located far from each other on the chromosome or on different chromosomes, may depend on the temperature. Then, i and j would be co-expressed if different individuals are sampled from living environments with different temperatures. Variation in ages of the individuals can similarly create co-expression among age-related genes. Alternatively, co-expression may originate from non-biological sources, such as technical or laboratory ones, whose exact origins are often unknown.

One is often interested in looking for differential co-expression, which refers to the different levels of gene co-expression between two phenotypically different sets of samples, such as a disease set versus a control set, or in two types of tissues [63, 65]. Differential co-expression often reveals information that one cannot obtain by examining differential expression (as opposed to co-expression), i.e., different levels of gene expression between the two sets of samples [73].

2.4 Metabolite networks

One can also construct correlation networks from metabolomics data [74, 75]. Like gene co-expression, correlation between metabolites can occur for multiple reasons, including knock-out of a gene coding an enzyme that is involved in a chemical reaction consuming or producing two metabolites, different temperatures or other environmental conditions under which different samples are obtained, or intrinsic variability owing to cellular metabolism [74]. Note that mass conservation within a moiety-conserved cycle produces negative correlation between at least one pair of metabolites involved in the reaction [76]. That said, in some cases one may consider correlation or other similarity between only a subset of metabolites that are not necessarily associated to one another by direct chemical processes but instead draw from a set of alternative biochemical processes (see, e.g., [77]).

2.5 Microbiome networks

Microbes interact with other microbe species as well as with their environments. Understanding of microbial composition and interaction in the human gut is expected to inform multiple diseases. Similarly, understanding soil microbial communities may contribute to enhancing plant productivity. Network analysis is adept at revealing, e.g., ecological community assembly and keystone taxa, and has been increasingly contributing to these fields.

In microbiome network analysis, one collects samples from, e.g., soil, at various time points or locations. Each sample from an environment (e.g., soil, gut, animal corpus, or water) contains various microorganisms with different quantities. Co-occurrence network analysis is increasingly common in this field, aided by an increasing amount and accuracy of data [26, 78, 79]. In a microbiome co-occurrence network, nodes are microorganisms (e.g., bacteria, archaea, or viruses), specified at the taxa level, for example, and an edge is defined to exist if two nodes co-occur across the samples. Therefore, microbiome co-occurrence networks are essentially microbiome correlation networks, and the usual correlation measures, such as Pearson correlation, can be used to determine edge data, but more sophisticated methods to define edges are more often used. (See [26, 78] for various co-occurrence network construction methods.) Positively weighted edges result because of, e.g., cooperation between two taxa, sharing of niche requirements, or co-colonization. Negatively edges result because of, e.g., competition for space or resources, prey-predator relationships,

¹A *phenotype* is a set of observable traits of an organism and is usually contrasted with the underlying *genotype* that causes (or influences) the phenotype.

or niche partitioning. A historically famous example of negative co-occurrence in ecological community assembly study is the checkerboard-like presence-absence patterns of two bird species inhabiting an island, discussed by Jared Diamond [80]. (Also see [26] for a historical account.) Regardless, one should keep in mind that correlation, or co-occurrence, does not immediately imply physical interaction between two taxa.

2.6 Disease networks

A node in a disease network is a disease phenotype. Correlation between two diseases defines an edge, and there are various definitions of edges as we introduce in this section. Each definition of edge creates a different type of disease network.

Comorbidity, also called multimorbidity [81], is the simultaneous occurrence of multiple diseases within an individual. One cause of comorbidity is that the same gene or disease-associated protein can trigger multiple diseases. Other causes, such as environmental factors or behaviors, such as smoking, can also result in comorbidity. A collection of potentially comorbid diseases can be modeled as the nodes of a network, and the edges, which are based on comorbidity or other similarity index between diseases [75], are correlational in nature.

The authors of [82] constructed phenotypic disease networks (PDNs) in which nodes are disease phenotypes. The edges are sample correlation coefficients or a variant, and the samples are patients in a hospital claim record (i.e., Medicare claims in the US). Note that here one uses correlation for binary variables because each sample (i.e., patient) is either affected or not affected by any disease i . The authors found that, for example, patients tend to develop illness along the edges of the PDN [82].

Similarly, prior work constructed a human disease network when two diseases share at least one associated gene, which is similar in principle to the phenotypic disease network despite that the edge of the human disease network is not a conventional correlation coefficient [83] (also see [84]). Similarly, an edge in a metabolic disease network is defined to exist when two diseases are either associated with the same metabolic reaction or their metabolic reactions are adjacent to each other in the sense that they share a compound that is not too common [85]. (H_2O and ATP, for example, are excluded because they are too common.) Alternatively, in a human symptom disease network [86], the edge between a pair of diseases is a correlation measure in which each sample is a symptom. In other words, roughly speaking, the edge weight is large when two diseases share many symptoms.

2.7 Financial correlation networks

Stocks of different companies are interrelated, and the prices of some of them tend to change similarly over time. A common transformation of such financial time series before constructing correlation matrices and networks is into the time series of logarithmic return, i.e., the successive differences of the logarithm of the price, given by

$$x_i(t) = \ln \frac{z_i(t+1)}{z_i(t)}, \quad (1)$$

where $z_i(t)$ is the price of the i th financial asset at time t , such as the closure price of the i th stock on day t , and $t \in \{0, \dots, T-1\}$. An advantage of this method is that $x_i(t)$ is not susceptible to changes in the scale of $z_i(t)$ over time [87]. Then, one constructs the correlation matrix for N time series $\{x_i(1), \dots, x_i(T-1)\}$, where $i \in \{1, \dots, N\}$.

Financial correlation matrices have been analyzed for decades. For example, Markowitz's portfolio theory provides an optimal investment strategy as vector $\mathbf{w} = (w_1, \dots, w_N)^\top$, where w_i represents the fraction of investment in the i th financial asset, and $^\top$ represents the transposition [5, 6]. The theory formulates the minimizer of the variance of the return, $\mathbf{w}^\top C \mathbf{w}$, where C is the covariance matrix, as the solution of a quadratic optimization problem with the constraint that the expected return, $\mathbf{w}^\top \mathbf{g}$, where $\mathbf{g} = (g_1, \dots, g_N)^\top$, and g_i is the expected return for the i th asset, is larger than a prescribed threshold.

Financial correlation matrices have also been extensively studied in econophysics research since the 1990s, with successful uses of random matrix theory [6, 87–93] and network methods such as maximum spanning trees [94] and more advanced methods (see [24] for a review). One usually employs random matrix theory in this context to verify that most eigenvalues of the empirical financial correlation matrices lie in the bulk part of the distribution of eigenvalues for random matrices. Such results imply that most eigenvalues of the empirical correlation matrices can be regarded as noise, and one is primarily interested in other dominant eigenvalues of the empirical correlation matrices whose values are not explained by random matrix theory [88–90]. The largest eigenvalue is usually not explained by random matrix theory and is often called the market mode.

Other types of financial data are possible. For example, correlation networks were constructed from pairwise correlation between the daily time series of the investor's behavior (i.e., the net volume of Nokia stock traded or its normalized version) for two investors [95, 96]. One can also renormalize the covariance matrix using other indices, such as momentum [97].

2.8 Bibliometric networks

Apart from microbiome studies, bibliometric and scientometric studies are another research field in which co-occurrence networks are often used [98,99]. For example, in an academic co-authorship network, a node represents an author, and an edge represents co-occurrence (i.e., collaboration) of two authors in at least one paper. One can weigh the edge according to the number of coauthored papers or its normalized variant [100]. While keeping authors as nodes, one can also create other types of co-occurrence networks, such as co-citation networks in which an edge connects two authors whose papers are cited together by a later paper, and keyword-based co-occurrence networks in which an edge connects two authors sharing keywords associated with their papers. Nodes of co-occurrence bibliometric networks can also be journals, institutions, research areas, and so forth. These co-occurrence networks are mathematically close to correlation networks and have been useful for understanding research communities and specialities, communication among researchers, interdisciplinarity, and the structure and evolution of science, for example.

Various other web-based information has also been analyzed as co-occurrence networks. For example, tags annotating posts in social bookmarking systems can be used as nodes of co-occurrence networks [101]. Two tags are defined to form an edge if both tags appear on the same post at least once. One can also use the number of the posts in which the two tags co-appear as the edge weight. Another example is co-purchase networks in online marketplaces, in which a node represents an item, and an edge represents that customers frequently purchase the two items together [102].

2.9 Climate networks

Climate can be analyzed as a network of interconnected dynamical systems [103–106]. In most analyses, the nodes of the network are equal-angle latitude-longitude grid points on the globe. However, such angular partitions lead to grid cells with geometric areas that vary with latitude, which in particular might lead to spurious correlations in the measured quantities, especially near the poles; such biases might be addressed either by a node splitting scheme that aims to obtain consistent weights for the network parameters [107], or by choosing instead to work on a grid with (possibly only approximately) equal grid cell areas [108]. Each node has, for example, a time series measurement of the pressure level, which represents wind circulation of the atmosphere. The edge between a pair of nodes is based on the correlation between the two time series. An early study showed that all nodes in tropic regions have large degree (i.e., the number of edges that a node has) regardless of the longitude, whereas only a small fraction of nodes in the mid-latitude regions had large degrees [103]. Climate networks have been further used for understanding mechanisms of climate dynamics and predicting extreme events. For example, early warning signals were constructed from the degree of the nodes and clustering coefficient for climate networks of the Atlantic temperature field [109]. The proposed early warning signals were effective at anticipating the collapse of Atlantic Meridional Overturning Circulation. See section 2.1 of [106] for more examples.

3 Methods for creating networks from correlation matrices

To apply network analysis to correlation matrix data, we need to generate a network from correlation data (usually in the form of a correlation matrix). We call such a network a *correlation network*. Whether correlation network analysis works or is justified depends on this process. Although there are various methods for constructing correlation networks from data, they have pros and cons. Furthermore, there are various unjustified practices around correlation network generation, which may yield serious limitations on the power of correlation network analysis. In this section, we review several major methods.

3.1 Estimation of covariance matrices

How to estimate covariance matrices from observed data when the matrix size is not small is a long-standing question in statistics and surrounding research fields. In particular, the sample covariance matrix, a most natural candidate, is known to be an unreliable estimate of the covariance matrix. See [6,110–112] for surveys on estimation of covariance matrices. Although the primary focus of this paper is estimation of correlation networks, not correlation or covariance matrices, we briefly survey a few techniques of covariance matrix estimation in this section, including providing the notations and preliminaries used in the remainder of this paper. This exposition is important in particular because correlation network analysis in non-statistical research fields such as network science and also various applications often ignores statistical perspectives examined in the previous studies.

We denote by $(x_{i\ell})$ an $N \times L$ data matrix, where N is the number of nodes to observe the signal from, and L is the number of samples, which is typically the length of the time series or the number of participants in an experiment or questionnaire. The sample covariance matrix, $C^{\text{sam}} = (C_{ij}^{\text{sam}})$, is given by

$$C_{ij}^{\text{sam}} = \frac{1}{L-1} \sum_{\ell=1}^L (x_{i\ell} - \bar{x}_i)(x_{j\ell} - \bar{x}_j), \quad (2)$$

where

$$\bar{x}_i = \sum_{\ell=1}^L \frac{x_{i\ell}}{L} \quad (3)$$

is the sample mean of the signal from the i th node.² Because Eq. (2) is essentially a spectral decomposition of C^{sam} , the rank of C^{sam} is at most L . One can understand this fact more easily by rewriting Eq. (2) as

$$C^{\text{sam}} = \frac{1}{L-1} \sum_{\ell=1}^L \tilde{\mathbf{x}}_{\ell} \tilde{\mathbf{x}}_{\ell}^{\top}, \quad (4)$$

where $\tilde{\mathbf{x}}_{\ell} = (x_{1\ell} - \bar{x}_1, \dots, x_{N\ell} - \bar{x}_N)^{\top}$. Therefore, C^{sam} is singular if $L < N$, while the converse does not hold true in general.

Let X_i denote a random variable for $i \in 1, \dots, N$. The true covariance matrix $C = (C_{ij})$ is given by

$$C_{ij} = E[(X_i - \mu_i)(X_j - \mu_j)], \quad (5)$$

where E represents the expectation, and $\mu_i = E[X_i]$ is the ensemble mean of X_i . In statistics, C^{sam} is regarded as an estimator of C , called the Pearson estimator. Equation (5) implies that a covariance matrix is a symmetric matrix. It is also a positive semidefinite matrix. Conversely, a symmetric positive semidefinite-matrix is always a covariance matrix.

For any finite L , the sample covariance matrix obeys the so-called Wishart distribution with L degrees of freedom, denoted by $W_N(L, C)$, under the assumption that the L samples are i.i.d. and obey the multivariate normal distribution whose covariance matrix is C [3, 6, 113, 114]. We obtain $E[C^{\text{sam}}] = C$. In other words, the sample covariance matrix is an unbiased estimator of the true covariance matrix. The variance of C_{ij}^{sam} is equal to $(C_{ij}^2 + C_{ii}C_{jj})/L$. In fact, C^{sam} is a problematic substitute of C , and the use of C^{sam} in applications in place of C tends to fail; see [6] for an example in portfolio optimization. An intuitive reason why C^{sam} is problematic is that, if L is not much larger than N , which is often the case in practice, one would need to estimate many parameters from a relatively few observations. Specifically, the covariance and correlation matrices have $N(N+1)/2$ and $N(N-1)/2$ unknowns to infer, respectively, whereas there are L samples of vector $(x_{1\ell}, \dots, x_{N\ell})$ available [115]. If N/L is not vanishingly small (called the large dimension limit or the Kolmogorov regime [6]), then the estimation would fail. As an extreme example, if $L < N$, then C^{sam} is singular, but C is in general nonsingular. Even if $L \geq N$, matrix C^{sam} may be ill-conditioned if L is not sufficiently greater than N , whereas C may be well-conditioned.

Therefore, covariance selection to reduce the number of parameters to be estimated is a recommended practice when L is not large relative to N [115]. One also says that we impose some structure on the estimator of the covariance matrix, with the mere use of the sample covariance matrix as an estimate of the true covariance matrix corresponding to no assumed structure.

A major method of covariance selection is to impose sparsity on the covariance matrix or the precision matrix (also called the condensation matrix), which is the inverse covariance matrix. Note that a sparse precision matrix does not imply that the corresponding covariance matrix (i.e., inverse of the precision matrix) is sparse. Graphical lasso (see section 3.6) is a popular method to estimate a sparse precision matrix. Another major method to estimate a sparse correlation matrix is to threshold on the value of the correlation to discard node pairs with correlation values close to 0 (see section 3.2). Another common method of covariance selection, apart from estimating a sparse covariance matrix, is covariance shrinkage (see [116] for a review). With covariance shrinkage, the estimated covariance matrix is a linear weighted sum of the sample covariance matrix, C^{sam} , and a much simpler matrix, called the shrinkage target, such as the identity matrix [117–119] or the so-called single-index model (which is a one-factor model in factor analysis terminology and is an approximation of C^{sam} by a rank-one matrix plus residuals) [117]. Note that the shrinkage target is a biased estimator of C . These and other covariance selection methods balance between the estimation biases and variances.

²Note the $L-1$ in the denominator of Eq. (2) is necessary to obtain an unbiased estimator.

We denote the correlation matrix by ρ . The sample Pearson correlation matrix, denoted by $\rho^{\text{sam}} = (\rho_{ij}^{\text{sam}})$ is defined by

$$\rho_{ij}^{\text{sam}} = \frac{\sum_{\ell=1}^L (x_{i\ell} - \bar{x}_i)(x_{j\ell} - \bar{x}_j)}{\sqrt{\sum_{\ell=1}^L (x_{i\ell} - \bar{x}_i)^2} \sqrt{\sum_{\ell=1}^L (x_{j\ell} - \bar{x}_j)^2}} = \frac{C_{ij}^{\text{sam}}}{\sqrt{C_{ii}^{\text{sam}} C_{jj}^{\text{sam}}}}. \quad (6)$$

Note that $\rho_{ii}^{\text{sam}} = 1 \forall i \in \{1, \dots, N\}$. Also note that every sample correlation matrix is a sample covariance matrix of some data but not vice versa.

A correlation matrix is characterized by positive semidefiniteness, symmetry, range of the entries only being $[-1, 1]$, and the diagonal being equal to 1 [120]. The set of full-rank correlation matrices for a fixed N is called the ellipsope, which has its own geometric structure [121, 122].

For standardized samples $y_{i\ell} = (x_{i\ell} - \bar{x}_i)/\sqrt{C_{ii}^{\text{sam}}}$, the Euclidean distance between vectors (y_{i1}, \dots, y_{iL}) and (y_{j1}, \dots, y_{jL}) is given by

$$d_{ij}^2 = \sum_{\ell=1}^L (y_{i\ell} - y_{j\ell})^2 = 2 - 2\rho_{ij}^{\text{sam}}. \quad (7)$$

Therefore, given the sample correlation matrix, $d_{ij} = \sqrt{2(1 - \rho_{ij}^{\text{sam}})}$ defines a Euclidean distance [87, 94].

3.2 Dichotomization

In this and the following subsections, we present several methods to generate undirected networks from correlation matrices.

A simple method to generate a network from the given correlation matrix is thresholding, which in its simplest form entails setting a threshold θ , and placing an unweighted edge (i, j) if and only if the Pearson correlation $\rho_{ij} \geq \theta$; otherwise, we do not include an edge (i, j) . It is also often the case that one thresholds on $|\rho_{ij}|$. There are mainly two choices after the thresholding. First, we may discard the weight of the surviving edges to force it to 1, creating an unweighted network. Second, we may keep the weight of the surviving edge to create a weighted network. See Fig. 1 for these two cases. The literature often use the term thresholding in one of the two meanings without clarification. In the remainder of this paper, we call the first case *dichotomizing* (which can be also called binarizing), which is, precisely speaking, a shorthand for “thresholding followed by dichotomizing”. We discuss dichotomized networks in this section and threshold networks without dichotomization (yielding weighted networks) in sections 3.3 and 3.6.

Dichotomizing has commonly been used across research areas. However, researchers have repeatedly pointed out that dichotomizing is not recommended for multiple reasons.

First, no consensus exists regarding the method for choosing the threshold value [27, 123–125] despite that results of correlation network analysis are often sensitive to the threshold value [124–128]. In a related vein, if a single threshold value is applied to the correlation matrix obtained from different participants in an experiment, which is typical in neuroimaging data analysis and referred to as an absolute threshold [124, 129], the edge density can vary greatly across participants. Since edge density is heavily correlated with many network measures, this can be seen as introducing a confound into subsequent analyses and casts doubt on consequent conclusions, e.g., that sick participants tend to have less small-world brain networks than healthy controls. (In this example, a network with a large edge density would in general yield a small average path length and large clustering coefficient, leading to the small-world property, so that density differences alone could have driven the observed effect.) An alternative method for setting the threshold is the so-called proportional thresholding, with which one keeps a fixed fraction of the strongest (i.e., most correlated) edges to create a network, separately for each participant [124, 129]; also see [130–132] for an early study. In this manner, the thresholded networks for different participants have the same density of edges. However, while the proportional thresholding may sound reasonable, it has its own problems [129]. First, because different participants have different magnitudes of overall correlation coefficient values, the proportional threshold implies that one includes relatively weakly correlated node pairs as edges for participants with an overall low correlation coefficients. This procedure increases the probability of including relatively spurious node pairs, which can be regarded as type I errors (i.e., false positives), increasing noise in the resulting network. (Also see [133, 134] for discussion on this matter.) Second, the overall correlation strength is often predictive of, for example, a disease in question. The proportional threshold enforces the same edge density for the different participants’ networks. Therefore, it gives up the possibility of using the edge density, which is a simplest network index, to account for the group difference. If one uses the absolute threshold, the edge density is different among participants, and one can use it to characterize participants. The edge density in the proportional thresholding is also an arbitrary parameter.

Second, apart from false positives due to keeping small-correlation node pairs as edges, correlation networks at least in its original form suffer from false positives because pairwise correlation does not differentiate between direct

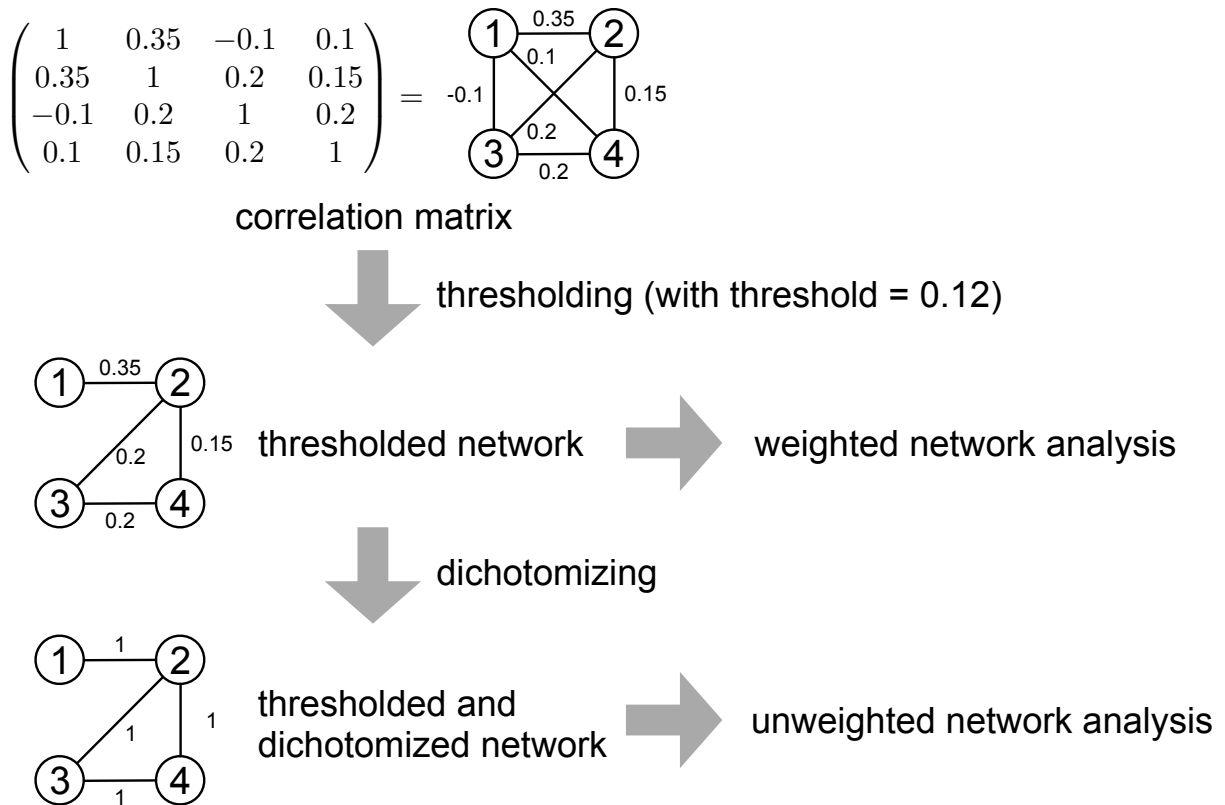


Figure 1: Thresholding a correlation matrix. We set the threshold at $\theta = 0.12$. If we only threshold the correlation matrix, we obtain a weighted network. If we further dichotomize the threshold matrix, we obtain an unweighted network. A different θ yields a different network in general.

effects (i.e., nodes i and j are correlated because they directly interact) and indirect effects (i.e., nodes i and j are correlated because i and k interact and j and k interact). In other words, correlations are transitive. The correlation coefficient is lower-bounded by [135]

$$\rho_{ij} \geq \rho_{ik}\rho_{jk} - \sqrt{(1 - \rho_{ik})^2(1 - \rho_{jk})^2}. \quad (8)$$

Equation (8) implies that if ρ_{ik} and ρ_{jk} are large, i.e., sufficiently close to 1, then ρ_{ij} is positive. Furthermore, this lower bound of ρ_{ij} is usually not tight, suggesting that ρ_{ij} tends to be more positive than what Eq. (8) suggests when $\rho_{ik}, \rho_{jk} > 0$ [136, 137]. This false positive problem is the main motivation behind the definition of the partial correlation networks and related methods with which to remove such a third-party effect, i.e., influence of node k in Eq. (8). (See section 3.5.) Instead, one may want to suppress false positives by carefully choosing a threshold value. Let us consider the absolute thresholding. For example, if i and j do not directly interact, i and k do, j and k also do, yielding $\rho_{ij} = 0.4$, $\rho_{ik} = 0.7$ and $\rho_{jk} = 0.6$, then setting $\theta = 0.5$ enables us to remove the indirect effect by k . However, it may be the case that i' and j' do not directly interact, i' and k' do, j' and k' also do, yielding $\rho_{i'j'} = 0.2$, $\rho_{i'k'} = 0.3$, and $\rho_{j'k'} = 0.4$. Then, thresholding with $\theta = 0.5$ dismisses direct as well as indirect interactions (that is, it introduces false negatives). A related artifact introduced by the combination of thresholding and indirect effects is that thresholding tends to inflate the abundance of triangles, as measured by the clustering coefficient, and other short cycles [74, 137]; even correlation networks generated by thresholding randomly and independently generated data $\{x_{i\ell}\}$ have high clustering coefficients [137]. This phenomenon resembles the fact that spatial networks tend to have high clustering just because the network is spatially embedded [138, 139].

Third, whereas thresholding has been suggested to be able to mitigate uncertainty on weak links (including the case of the proportional thresholding to some extent) and enhance interpretability of the graph-theoretical results (e.g., [27]), thresholding in fact discards the information contained in the values of the correlation coefficient. For example, in Fig. 1, thresholding turns a correlation of -0.1 and 0.1 into the absence of an edge. Furthermore, if we dichotomize the edges that have survived thresholding, a correlation of 0.2 and 0.35 are both turned into the presence of an edge.

There are various methods to try to mitigate some of these problems. In the remainder of this section, we cover methods related to dichotomizing.

One family of solutions is to integrate network analysis results obtained with different threshold values [27] (but see [140] for a critical discussion). For example, one can calculate a network index, such as the node's degree, denoted by α , as a function of the threshold value, θ , and fit a functional form to the obtained function $\alpha(\theta)$ to characterize the node [127]. Similarly, one can calculate α for a range of θ values and take an average of α [141, 142]. In the case of group-to-group comparison, an option along this line of idea is the functional data analysis (FDA), with which one looks at α as a function of θ across a range of θ values and statistically test the difference between the obtained function for different groups by a nonparametric permutation test [143, 144]. In these methods, how to choose the range of θ is a nontrivial question.

A different strategy is to determine the threshold value according to an optimization criterion. For example, a method was proposed [125] for determining the threshold value as a solution of the optimization of the trade-off between the efficiency of the network [145] and the density of edges. Another method to set θ is to use the highest possible threshold that guarantees all or most (e.g., 99%) of nodes are connected [146].

The maximal spanning tree is an easy and classical method to automatically set the threshold and guarantee that the network is connected [94]. One adds the largest correlation node pairs as edges one by one under the condition that the generated network is the tree. In the end, the maximal spanning tree contains all the N nodes, and the number of edges is $N - 1$. The maximal spanning tree also allows a hierarchical tree representation, which facilitates interpretation [94, 147, 148]. However, the generated network is extreme in the sense that it is a most sparse network among all the connected networks on N nodes, without any triangles. A variant of the maximum spanning tree is to sequentially add edges with the largest correlation value under the constraint that the generated network can be embedded on a surface of a prescribed genus value (roughly speaking, the given number of holes) without edge intersection [149]. If the genus is constrained to be zero, the resulting network is a planar graph, called the planar maximally filtered graph (PMFG). The PMFG contains $3N - 6$ edges. The PMFG contains more information than the maximum spanning tree, such as some cycles and their statistics. Another related method is to use the k nearest neighbor graph of the correlation matrix, with which each i th node is connected at least to the k nodes with the highest correlation with the i th node [134]. Yet another choice, which is designed for general weighted networks, is the disparity filter, with which one preserves only statistically significant edges to generate the *network backbone* [150]. Note that, with these methods, some lower-correlation node pairs are retained as edges and some higher-correlation edges are discarded.

3.3 Weighted networks

A strategy for avoiding the arbitrariness in the choice of the threshold value and loss of information in dichotomizing is to use weighted networks, retaining the pairwise correlation value as the edge weight [60, 123]. Although there are numerous settings in network science where negative edge weights are considered, they are generally more difficult to treat. (See section 3.4.) As such, two common methods to create positively weighted networks are (1) using the absolute value of the correlation coefficient as the edge weight and (2) ignoring negatively weighted edges and only using the positively weighted edges. Both methods dismiss some information contained in the original correlation matrix, i.e., the sign of the correlation or the magnitude of the negative pairwise correlation. Nonetheless, these transformations are widely used because many methods are available for analyzing general positively weighted networks, many of which are extensions of the corresponding methods for unweighted networks. One can also use methods that are specifically designed for weighted networks [151].

It should be noted that weighted networks share the problem of false positives due to indirect interaction between nodes with the unweighted networks created by dichotomization. We also note that, in contrast to thresholding (which may be followed by dichotomization), node pairs with any small correlation (i.e., correlation coefficient close to 0) are kept as edges in the case of the weighted network. This may increase the uncertainty of the generated network and hence of the subsequent network analysis results.

Thresholding operations in statistics literature to increase the sparsity of the estimated covariance matrix often produce weighted networks. This is in contrast to the dichotomization, which produces unweighted networks. Hard thresholding in statistics literature refers to coercing C_{ij}^{sam} , with $i \neq j$, to 0 if $|C_{ij}^{\text{sam}}| < \theta$ and keep the original C_{ij}^{sam} if $|C_{ij}^{\text{sam}}| \geq \theta$ [110, 152–154]. Soft thresholding [152, 154, 155] transforms C_{ij}^{sam} by a continuous non-decreasing function of C_{ij}^{sam} , denoted by $f(C_{ij}^{\text{sam}})$, such that

$$f(x) = \begin{cases} x - \theta & (x \geq \theta), \\ 0 & (-\theta < x < \theta), \\ x + \theta & (x \leq -\theta). \end{cases} \quad (9)$$

This assumption implies that, in contrast to hard thresholding, there is no discontinuous jump in the transformed edge weight at $C_{ij}^{\text{sam}} = \pm\theta$. Both hard and soft thresholding, as well as a more generalized class of thresholding function $f(x)$ [154], do not imply dichotomization and therefore generate weighted networks. In numerical simulations, all these thresholding methods to generate weighted networks outperformed the sample covariance matrix in estimating true sparse covariance matrices [154]. The same study also found that there was no clear winner between hard or soft thresholding, while combination of them tended to perform somewhat better than other types of thresholding. Adaptive thresholding refers to using threshold values that depend on (i, j) . Adaptive thresholding performs better in terms of the approximation error and theoretically converges faster than universal thresholding schemes (i.e., using a threshold value independent of (i, j)) in numerical simulations [156].

3.4 Negative weights

Correlation matrices have negative entries in general. In the case of both unweighted and weighted correlation networks, we often prohibit negative edges either by coercing negative entries of the correlation matrix to zero or by taking the absolute value of the pairwise correlation before transforming the correlation matrix into a network. We prohibit negative edges for two main reasons. First, in some research areas, it is often difficult to interpret negative edges. In the case of multivariate financial time series, a negative edge implies that the price of the two assets tend to move in the opposite manner, which is not difficult to interpret. In contrast, when fMRI time series from two brain regions are negatively correlated, it does not necessarily imply that these regions are connected by inhibitory synapses, and it is not straightforward to interpret negative edges in brain dynamics data [27, 157]. Second, compared to weighted networks and directed networks, we do not have many established tools for analyzing networks in which positive and negative edges are mixed, i.e., signed networks. Signed network analysis is still emerging [158].

In fact, negative edges may provide useful information. For example, they benefit community detection because, while many positive edges should be within a community, negative edges might ideally connect different communities rather than lie within a community. Some community detection algorithms for signed networks exploit this idea [158, 159]. Another strategy for analyzing signed network data is to separately analyze the network composed of positive edges and that composed of negative edges and then combine the information obtained from the two analyses. For example, the modularity, an objective function to be maximized for community detection, can be separately defined for the positive network and the negative network originating from a single signed network and then combined to define a composite modularity to be maximized [123, 160]. While these methods are designed for general signed networks, they have been applied to brain correlation networks [123, 159].

Another type of approach to signed weighted networks is nonparametric weighted stochastic block models [161, 162], which are useful for modeling correlation matrix data. Crucially, this method separately estimates the unweighted network structure and the weight of each edge but in a unified Bayesian framework. By imposing a maximum-entropy principle with a fixed mean and variance on the edge weight, they assumed a normal distribution for the signed edge weight. Because the edge weight in the case of correlation matrices, i.e., the correlation coefficient, is confined between -1 and 1 , an ad-hoc transformation to map $(-1, 1)$ to $(-\infty, \infty)$ such as $y = 2 \operatorname{arctanh} x = \ln \frac{1+x}{1-x}$ is applied before fitting the model. One can assess the goodness of such an ad-hoc transformation by a posteriori comparison with different forms of functions to transform x to y using Bayesian model selection [162]. In this way, this stochastic block model can handle negative correlation values. With this method, one can determine community structure (i.e., blocks) including its number and hierarchical structure.

3.5 Partial correlation

A natural method with which to avoid false positives due to indirect interaction effects in the Pearson correlation matrix is to use the partial correlation coefficient (as in, e.g., [163–165]). This entails measuring the linear correlation between nodes i and j after partialing out the effect of the other $N - 2$ nodes. Specifically, to calculate the partial correlation between nodes i and j , we first compute the linear regression of X_i on $\{X_1, \dots, X_N\} \setminus \{X_i, X_j\}$, which we write as $X_i \approx \sum_{m=1; m \neq i, j}^N \beta_{i,m} X_m$, where $\beta_{i,m}$ is the coefficient of linear regression. Similarly, we regress X_j on $\{X_1, \dots, X_N\} \setminus \{X_i, X_j\}$, which we write as $X_j \approx \sum_{m=1; m \neq i, j}^N \beta_{j,m} X_m$. The residuals for L samples are given by $\varepsilon_{i,\ell} = x_{i\ell} - \sum_{m=1; m \neq i, j}^N \beta_{i,m} x_{m\ell}$ and $\varepsilon_{j,\ell} = x_{j\ell} - \sum_{m=1; m \neq i, j}^N \beta_{j,m} x_{m\ell}$, where $\ell \in \{1, \dots, L\}$. The partial correlation coefficient, denoted by $\bar{\rho}_{ij}^{\text{par}}$, is the Pearson correlation coefficient between $\{\varepsilon_{i,1}, \dots, \varepsilon_{i,L}\}$ and $\{\varepsilon_{j,1}, \dots, \varepsilon_{j,L}\}$.

In fact, the partial correlation coefficient between i and j ($j \neq i$) is given by

$$\bar{\rho}_{ij}^{\text{par}} = -\frac{\Omega_{ij}}{\sqrt{\Omega_{ii}\Omega_{jj}}}, \quad (10)$$

where $\Omega = C^{-1}$ is the precision matrix [113, 114]. Equation (10) implies that $\Omega_{ij} = 0$ is equivalent to the lack of partial correlation, i.e., $\bar{\rho}_{ij}^{\text{par}} = 0$. This conditional independence property gives an interpretation of the precision matrix, Ω .

Equation (10) also implies that the partial correlation can be calculated only when C is of full rank, whose necessary but not sufficient condition is $L \geq N$. If C is rank-deficient, a natural estimator of the $N \times N$ partial correlation matrix $\bar{p}^{\text{par}} = (\bar{\rho}_{ij}^{\text{par}})$ is a pseudoinverse of C . However, the standard Moore-Penrose pseudoinverse is known to be a suboptimal estimator in terms of approximation error [166, 167], while the pseudoinverse is useful for screening for hubs in partial correlation networks [167]. If C is of full rank, Ω as well as C is positive definite. Therefore, \bar{p}^{par} , whose diagonal entries are forced to be -1 , is negative definite. We can verify this by rewriting Eq. (10) as $\bar{p}^{\text{par}} = -D^{-1/2}\Omega D^{-1/2}$, where $D = \operatorname{diag}(\Omega_{11}, \dots, \Omega_{NN})$ is the diagonal matrix whose diagonal entries are $\Omega_{11}, \dots, \Omega_{NN}$. If we consider matrix $2I + \bar{p}^{\text{par}}$, where I is the identity matrix, as an alternative partial correlation matrix to force its diagonal entries to 1 instead of -1 , the eigenvalues of the new partial correlation matrix are upper-bounded by 2 [168].

By thresholding the partial correlation matrix, or using an alternative method, one obtains an unweighted or weighted partial correlation network, depending on whether we further dichotomize the thresholded matrix. Because the partial correlation avoids the indirect interaction affect, the network created from random partial correlation matrices yields, for example, smaller clustering coefficients [137] than if we had used the Pearson correlation matrix.

While it apparently sounds reasonable to partial out the effect of the other nodes to determine a pairwise correlation between two nodes, it is not straightforward to determine when the partial correlation matrix is better than the Pearson correlation one. First, Eq. (10) implies that extreme eigenvalues of \bar{p}^{par} are those of a normalized precision matrix. Because the precision matrix is the inverse of the covariance matrix C , extreme eigenvalues of \bar{p}^{par} are derived from eigenvalues of C with small magnitudes. It is empirically known for, e.g., financial time series, that small-magnitude eigenvalues of the covariance matrices are buried in noise, i.e., not distinguishable from eigenvalues of random matrices [88, 89]. Therefore, the dominant eigenvalue of the precision matrix is strongly affected by noise [169].

Second, the entries of \bar{p}^{par} are more variable than those of Pearson correlation matrices. Specifically, if (x_1, \dots, x_N) obeys a multivariate normal distribution, the Fisher-transformed partial correlation of a sample partial correlation, i.e.,

$$z_{ij} = \frac{1}{2} \ln \left(\frac{1 + \bar{\rho}_{ij}^{\text{par}, \text{sam}}}{1 - \bar{\rho}_{ij}^{\text{par}, \text{sam}}} \right), \quad (11)$$

where $\bar{\rho}_{ij}^{\text{par,sam}}$ is the sample partial correlation calculated through Eq. (10) with $\Omega = (C^{\text{sam}})^{-1}$, approximately obeys the normal distribution with mean $\frac{1}{2} \ln \left(\frac{1+\bar{\rho}_{ij}^{\text{par}}}{1-\bar{\rho}_{ij}^{\text{par}}} \right)$ and standard deviation $[L-3-(N-2)]^{-1/2}$. This result dates back to Fisher (see e.g., [170]). In contrast, the corresponding result for the Fisher transformation of the Pearson correlation coefficient is that the transformed variable approximately obeys the normal distribution with mean $\frac{1}{2} \log \left(\frac{1+\rho_{ij}^{\text{sam}}}{1-\rho_{ij}^{\text{sam}}} \right)$ and standard deviation $(L-3)^{-1/2}$ [170]. Therefore, the partial correlation has more sampling variance than the Pearson correlation unless $L \gg N$.

Third, partial correlation matrices typically have more negative entries and smaller-magnitude entries than Pearson correlation matrices [170,171]. Combined with the larger variation of the sample partial correlation than the sample Pearson correlation discussed just above, the tendency that $\bar{\rho}_{ij}^{\text{par}}$ has a smaller magnitude than ρ_{ij} poses a challenge of statistically validating the estimated partial correlation networks [170].

3.6 Graphical lasso and variants

Estimating a true correlation matrix, which contains $N(N-1)/2$ unknowns, is an ill-founded problem unless the number of samples is sufficiently larger than $N(N-1)/2$. A strategy to overcome this problem is to impose sparsity of the estimated correlation network. A sparsity constraint enforces zeros on a majority of matrix entries to suppress the number of unknowns to be estimated relative to the number of samples. Imposing sparsity on estimated correlation networks is a major form of covariance selection. *Structural learning* refers to estimation of an unknown network from data and usually assumes that the given data obey a multivariate normal distribution and that the estimated network is sparse. For a review with tutorials on this topic, see [38].

The Gaussian graphical model assumes that the precision matrix from the data obeys a multivariate normal distribution and usually imposes sparsity of the precision matrix [114]. In addition to reducing the number of unknowns to be estimated, a motivation behind estimating a sparse precision matrix is that $\Omega_{ij} = 0$ is equivalent to the absence of conditional linear dependence of the signals at the i th and j th nodes given all the other $N-2$ variables, which is easy to interpret. The graphical lasso is an algorithm for learning the structure of a Gaussian graphical model [172–178]. The graphical lasso maximizes the likelihood of the multivariate normal distribution under a lasso penalty (i.e., ℓ_1 penalty), whose simplest version is of the form $\lambda \sum_{i,j=1}^N |\Omega_{ij}|$, where we recall that Ω_{ij} is the (i,j) entry of the precision matrix, and λ is a positive constant. This penalty term is added to the negative log likelihood to be minimized. If λ is large, it strongly penalizes positive $|\Omega_{ij}|$, and the minimization of the objective function yields many zeros of the estimated Ω_{ij} . One can extend the lasso penalty function in multiple ways, for example, by allowing λ to depend on (i,j) and automatically determining λ using an information criterion. Other ways to regularize the number of nonzero elements in the precision matrix than lasso penalty are also possible. (See e.g., [179–181].)

An alternative to the graphical lasso is to estimate sparse covariance matrices rather than sparse precision matrices under lasso penalty [182–186]. With this approach, the consequence of imposing sparsity, $C_{ij} = 0$, corresponds to marginal independence between X_i and X_j .

Most graphical lasso models and their variants do not model the estimation problem relative to a null model correlation matrix. However, by estimating a sparse correlation matrix that is different relative to a null model of correlation matrix (see section 3.8 for null models), it was found that the estimated correlation matrix gives a better description of the given financial correlation matrix data than the graphical lasso and that the choice of the null model also affects the performance [186]. By construction, this method infers a set of edges that are not expected from the so-called correlation matrix configuration model (see section 3.8 for details).

A test of significance of an edge, run on each edge, may sound like a natural way to filter a network. However, this idea is not feasible because multiple comparison with $N(N-1)/2$ estimates, each of whose significance would have to be tested, is not practical given that $N(N-1)/2$ is usually large [38] and also because the different edges are correlated with each other, particularly if they share a node. Rather, the edges that survive the filtering method, such as the graphical lasso, should be regarded to be sufficiently strong to be included in the model [38].

3.7 Temporal correlation networks

Many empirical networks vary over time, including temporal correlation networks [187], and many methods have been developed for analyzing time-varying network data [187–190]. If the given data is a multivariate time series that is non-stationary, then correlation matrices computed from the first 10% of the time points may be drastically different from that computed from the last 10%. So, there is the possibility of greater adaptability and better generalizability when one uses a time series of correlation networks rather than just one. One can then apply various temporal network analysis tools to the obtained temporal correlation networks.

A simple method to create dynamic correlation networks from multivariate time series data is sliding-window correlation [191] (also called rolling-window correlation in the finance literature; see e.g. [192]). With this method, one considers time windows within the entire observation time horizon, $t = \{1, \dots, t_{\max}\}$. These time windows may be overlapping or non-overlapping. Then, within each time window, one calculates the correlation matrix and network. If there are 100 time windows within $[1, t_{\max}]$, then this method creates a temporal network of length 100. Reliably computing a single correlation matrix and a static correlation network from multivariate time series requires a reasonable length (i.e., the number of time points) of a time window. Generation of a reliable dynamic correlation network requires longer data because one needs a multitude of such reasonably long time windows. A limitation of sliding-window correlations is that they are susceptible to large variability if the size of the time window is small, whereas a large window size sacrifices sensitivity to temporal changes [193].

Early seminal reports analyzed temporal correlation networks of stock markets by tracking financial indices and central nodes of the static correlation network over more than a decade [148, 194, 195]. However, methods of dynamic correlation networks have been particularly developed in brain network analysis. In neuroimaging studies, in particular in fMRI studies, dynamic correlation networks are known as dynamic (or time-varying) functional connectivity networks [191, 196–199]. Temporal changes in functional (i.e., correlational) brain networks may represent neural signaling, behavioral performance, or changes in the cognitive state, for example. Patterns of time-varying functional networks may alter under a disease. One can also analyze stability of community structure of temporal correlation networks over time [200–202]. (See also [190] for temporal community detection in financial correlation networks.) Many variations of the method, such as on how to create sliding windows and how to cluster time windows to define discrete-state transition dynamics, and change-point detection are available in the field (e.g., see [199]). Many of these methods should be applicable to multivariate time series data to generate temporal correlation networks in other domains.

There are also methods for estimating dynamic precision matrices, proposed outside neuroscience [203–205]. For example, the time-varying graphical lasso (TVGL) formulates the inference of discrete-time time-varying precision matrix as a convex optimization problem [205]. The objective function is composed of maximization of the log likelihood under a lasso sparsity constraint and the constraint that the precision matrix at adjacent time points does not change too drastically, enforcing the temporal consistency.

3.8 Null models

A good practice to verify any structural or dynamical measurement α is to compare the value of α in the given network with the value of α achieved in random networks. This allows one to determine whether the α value measured for the given network data is explainable purely by the gross structural properties (e.g. edge density, degree distributions) of the random graph family (when the α value is similar between the given and random networks) or it is the result of other distinctive features of the data (when the α value is statistically different between the given and random networks). Many discoveries in network science owe to the fact that key analyses have prudently implemented this practice by using or inventing appropriate null models of networks. Already in one of the earliest seminal papers on small-world networks, Watts and Strogatz compared the average path length and the clustering coefficient of empirical networks with those of the Erdős-Rényi random graph having the same number of nodes and edges [206].

One of the most popular null models for networks is the configuration model, i.e., a uniform ensemble of networks under the constraint that the degree of each node is conserved [207, 208], either exactly or in expectation. By comparing given networks against a configuration model, one can reliably quantify and discuss various network properties such as network motifs [209], community structure [210], rich clubs [211], and core-periphery structure [212]. The rationale behind the use of the configuration model is that the node’s degree is heterogeneously distributed for many empirical networks and that one generally wants to explore structural, dynamical, or other properties of networks that are not immediate outcomes of the heterogeneous degree distribution. One can extend the configuration model by imposing additional constraints that the network under discussion is supposed to satisfy, such as spatiality, i.e., the constraint that the nodes are embedded in a metric space and the probability of an edge depends on the distance between the two nodes [213]. See [207, 214, 215] for reviews of configuration models and best practices for generating random realizations from such models.

We should similarly test properties found for given correlation networks against appropriate null models. However, the usual configuration models are not appropriate as null models of correlation networks because they are significantly different from correlation networks derived from purely random data [74, 90, 137, 190]. The expectation $\langle A_{ij} \rangle$ of the (i, j) entry of the adjacency matrix of the configuration model conditioned on the degrees of all nodes, at least in the idealized and unrealistic regime of weak heterogeneity of the degrees [214, 215], is equal to

$$\langle A_{ij} \rangle = \frac{k_i k_j}{Nk}, \quad (12)$$

where $k_i = \sum_{j=1}^N A_{ij}$ is the degree of the i th node in the original network, A_{ij} is the entry of the *empirical* adjacency matrix of the original network (i.e., $A_{ij} = 1$ if there is an edge between the i th and j th nodes, and $A_{ij} = 0$ otherwise), and \bar{k} is the average degree over all nodes. The above expected value also represents the probability of independently connecting the i th and j th nodes in realizations of the configuration model for networks. Note that, one can indeed realize graphs in the configuration model by sampling edges independently (at least if the constraint on the degree is ‘soft’, i.e. realized only as an ensemble average over realizations [215]), correlation matrices cannot be generated with independent entries, even in the null model of independent signals. This is because, even under the null hypothesis of independent realizations of the original time series, the correlation matrix constructed from such time series still obeys the ‘metric’ (or triangular) inequality in (8). We will elaborate more on this point below.

To see what Eq. (12) yields by merely replacing an empirical adjacency matrix with an empirical correlation matrix ρ_{ij} , we proceed as follows [90]. We assume that each empirical signal is standardized in advance such that $\text{Var}(X_i) = 1, \forall i \in \{1, \dots, N\}$. In this way, we do not need to distinguish between the correlation (i.e., ρ_{ij}) and covariance (i.e., C_{ij}) matrices. We express the ‘degree’ as

$$k_i = \sum_{j=1}^N \rho_{ij} = \sum_{j=1}^N C_{ij} = \sum_{j=1}^N \text{Cov}(X_i, X_j) = \text{Cov}(X_i, X_{\text{tot}}), \quad (13)$$

where Cov represents the covariance and $X_{\text{tot}} = \sum_{i=1}^N X_i$ is the ‘total’ signal. Then, we obtain

$$N\bar{k} = \sum_{i=1}^N k_i = \text{Cov}(X_{\text{tot}}, X_{\text{tot}}) = \text{Var}(X_{\text{tot}}), \quad (14)$$

where $\text{Var}(X_{\text{tot}})$ is the variance of X_{tot} . By inserting the above quantities into (12) with A_{ij} replaced by ρ_{ij} , we obtain for the expected correlation matrix

$$\langle \rho_{ij} \rangle = \frac{\text{Cov}(X_i, X_{\text{tot}})\text{Cov}(X_j, X_{\text{tot}})}{\text{Var}(X_{\text{tot}})} = \frac{\text{Cov}(X_i, X_{\text{tot}})}{\sqrt{\text{Var}(X_{\text{tot}})}\sqrt{\text{Var}(X_i)}} \cdot \frac{\text{Cov}(X_j, X_{\text{tot}})}{\sqrt{\text{Var}(X_{\text{tot}})}\sqrt{\text{Var}(X_j)}} = \rho(X_i, X_{\text{tot}})\rho(X_j, X_{\text{tot}}). \quad (15)$$

Technically, this expected matrix is a covariance matrix because it is symmetric, rank 1, and the only nonzero eigenvalue is positive [90,216]. To interpret the meaning of the above expression for $\langle \rho_{ij} \rangle$, we recall the definition of the conditional three-way partial Pearson correlation coefficient [3,113]:

$$\rho(X_i, X_j | X_{\text{tot}}) = \frac{\rho(X_i, X_j) - \rho(X_i, X_{\text{tot}})\rho(X_j, X_{\text{tot}})}{\sqrt{1 - \rho(X_i, X_{\text{tot}})^2}\sqrt{1 - \rho(X_j, X_{\text{tot}})^2}}. \quad (16)$$

We therefore conclude that the expected correlation matrix in (15) is a correlation matrix of N signals that satisfy the conditional independence relationship

$$\rho(X_i, X_j | X_{\text{tot}}) = 0 \quad (17)$$

$\forall i, j (\neq i) \in \{1, \dots, N\}$ [190].

However, when one generates a correlation network from the configuration model, i.e. from a correlation matrix obeying (17), the generated network is far from a typical correlation network generated by random data, due to the triangular inequality mentioned above. To see an example of this, let us revisit the example briefly explained in section 3.2. Let us consider purely random data in which we generate each sample $x_{i\ell}, i \in \{1, \dots, N\}, \ell \in \{1, \dots, L\}$ (where we recall that L is the number of samples for each node) as i.i.d. random numbers obeying a given normal distribution. Then, we calculate the correlation matrix for $\{x_{i\ell}\}$ and then a correlation network. For a broad class of methods, including thresholding, the generated correlation network has a high clustering coefficient [137], precisely because of the inequality (8). Therefore, high clustering coefficients in correlation networks should not come as a surprise. In contrast, networks generated by the ordinary configuration model yield low clustering coefficients [217], disqualifying it as a null model for correlation networks. If we use the usual configuration model as the null model, we would incorrectly conclude that a given correlation network has high clustering even if the network does not have particularly high clustering among correlation networks. The configuration model as null model also underperforms the simpler null model, called the uniform null model (which is analogous to the random regular graph and to the Hirschberger-Qi-Steuer (H-Q-S) algorithm explained below) on benchmark problems of community detection when communities of different sizes are present in single networks and those communities are detected by modularity maximization [190].

Several papers have noted the need for null models specifically for correlation networks [26,90,137,208,218]. We should use correlation networks derived from a random correlation matrix as a null model. We stress once again that

a random correlation matrix is different from a random network model (e.g., Erdős-Rényi model or configuration model), because of the dependencies between entries. Similarly, many classes of random matrices are not appropriate null models for correlation networks, either. For example, a symmetric matrix whose all on-diagonal entries are 1 and off-diagonal entries are i.i.d. uniformly on $(-1, 1)$ is almost never a correlation matrix unless N is small [219]. In this section, we introduce several null models of correlation matrices. All the null models presented give distributions over correlation matrices. Then, using any method introduced in previous sections (e.g., by thresholding in various ways), one can define corresponding null models over correlation networks.

A straightforward and traditional null model consists in shuffling the original data, $\{x_{i\ell}\}$, based on which the correlation matrix is calculated. This method is especially typical for multivariate time series data. For example, one preserves the power spectrum of the time series at each node while the time series is otherwise randomized [137, 208, 220, 221]. More specifically, one Fourier transforms the time series at the i th node, randomize the phase, and carry out the inverse Fourier transform. Then, for the randomized multivariate time series, one calculates the correlation matrix, which we use as control. One can impose additional constraints on the randomization of time series depending on the properties other than the power spectrum that one wants to have the null model preserve [222].

Another null model is based on the expected spectral properties of a correlation matrix, rather than on the expected matrix itself. Note that the expected correlation matrix, under the null hypothesis of independent signals, is the identity matrix whose entries we denote as $\rho_{ij}^{\text{MG1}} = \delta_{ij}$ (where δ_{ij} is the Kronecker delta symbol) [90, 190]. This null model corresponds to an expectation under white noise signals $\{x_{i\ell}\}$ that are independent for different nodes $i \in \{1, \dots, N\}$ and samples $\ell \in \{1, \dots, L\}$. However the sample pairwise correlation ρ_{ij}^{sam} measured from the signals, even under the null hypothesis of independence, will be different from the identity matrix, unless $L \rightarrow \infty$. To take into account the effects of finite L , it is convenient to look at the spectrum of the sample correlation matrix. If we assume a standardized independent normal distribution for $x_i \forall i$, then ρ^{sam} obeys the Wishart distribution $W_N(I, L)$, where we recall that I is the $N \times N$ identity matrix, the covariance matrix of a white noise signal. Note that the expectation of $W_N(I, L)$ is I . Early studies of financial multivariate time series data found that only a small number of the largest eigenvalues of the covariance matrix deviate from the distribution of eigenvalues predicted by random matrix theory for the Wishart ensemble [88, 89]. In other words, only the leading eigenvalues and the associated eigenvectors outside the prediction of random matrix theory, often called the market modes, are significant relative to the random matrix null model. Random matrix theory has provided useful null models for covariance/correlation matrix data, in particular in financial time series data analysis; see [6] for a review. Also see [120] for a review of random correlation as opposed to covariance matrices.

Among many possible specific choices of null models for correlation matrices based on random matrix theory, here we consider two models, which we denote by ρ^{MG2} and ρ^{MG3} , proposed in [90]. A given correlation matrix is symmetric and positive semidefinite and therefore can be decomposed as

$$\rho^{\text{sam}} = \sum_{i=1}^N \lambda_i \mathbf{u}_{(i)} \mathbf{u}_{(i)}^\top, \quad (18)$$

where $\lambda_i (\geq 0)$ is the i th eigenvalue of ρ^{sam} , and $\mathbf{u}_{(i)}$ is the associated normalized right eigenvector. The null model correlation matrix ρ^{MG2} preserves the contribution of small eigenvalues to Eq. (18), which are regarded to be noisy and described by random matrix theory, and is given by

$$\rho^{\text{MG2}} = \sum_{i=1; \lambda_i \leq \lambda_+}^N \lambda_i \mathbf{u}_{(i)} \mathbf{u}_{(i)}^\top, \quad (19)$$

where

$$\lambda_+ = \left(1 + \sqrt{\frac{N}{L}}\right)^2. \quad (20)$$

The boundary λ_+ originates from the Marchenko-Pastur distribution (also known as the Sengupta-Mitra distribution) and represents the expected largest eigenvalue under the null hypothesis of independent signals. Matrix ρ^{MG2} is not a correlation matrix because its diagonal elements are not equal to 1. However, this does not affect most network analysis because we usually ignore diagonal elements or self-loops in correlation networks. Matrix ρ^{MG2} represents a null model constructed only from the eigenvalues of the empirical correlation matrix that are deemed to be noisy. Therefore comparing the empirical matrix against ρ^{MG2} singles out properties that cannot be traced back to noise [90]. By contrast, matrix ρ^{MG3} also preserves the contribution of the largest eigenvalue (if all the entries of the associated

eigenvector is positive) in addition to that of the noisy eigenvalues and is given by

$$\rho^{\text{MG3}} = \lambda_{\max} \mathbf{u}_{(\max)} \mathbf{u}_{(\max)}^\top + \sum_{i=1; \lambda_i \leq \lambda_+}^N \lambda_i \mathbf{u}_{(i)} \mathbf{u}_{(i)}^\top, \quad (21)$$

where max is the index for the dominant eigenvalue of ρ^{sam} . All the entries of the dominant eigenvector, $\mathbf{u}_{(\max)}$, is positive if there is a sufficiently strong common trend affecting all the N signals. If this common trend is so strong that all the entries of the correlation matrix are positive, the Perron-Frobenius theorem ensures the positivity of the dominant eigenvector. When this happens, the common trend obscures all the mutual correlations among the signals. Matrix ρ^{MG3} deliberately removes this global trend in addition to the noise, to reveal the underlying structure. Therefore, properties of correlation matrices or correlation networks that are not expected from ρ^{MG3} represent those not anticipated by the simultaneous presence of local noise and global trends. In other words, they reflect the presence of mesoscopic correlated structures such as correlation-induced communities [90]. As we will discuss in section 4.2, one can indeed use matrix ρ^{MG3} to successfully detect communities of correlated signals.

As another null model, the H-Q-S algorithm, invented by Hirschberger, Qi, and Steuer [223] is an equivalent of the Erdős-Rényi random graph in general network analysis. Specifically, given the covariance matrix, C^{sam} , the H-Q-S algorithm generates random covariance matrices, C^{HQS} , under the following constraints. First, the expectation of each on-diagonal entry of C^{HQS} is equal to the average of the N on-diagonal entries of C^{sam} , denoted by $\mu_{\text{on}} \equiv (1/N) \times \sum_{i=1}^N C_{ii}^{\text{sam}}$. Second, the expectation and variance of each off-diagonal entry of C^{HQS} are equal to those of C^{sam} calculated on the basis of all the off-diagonal entries, denoted by μ_{off} and σ_{off}^2 , respectively. Optionally, one can also constrain the variance of the on-diagonal entries of C^{HQS} [223] or use a fine-tuned heuristic variant of the algorithm [137]. To implement the most basic H-Q-S algorithm without constraining the variance of the on-diagonal entries of C^{HQS} , we set

$$L^{\text{HQS}} \equiv \max(2, \lfloor (\mu_{\text{on}}^2 - \mu_{\text{off}}^2) / \sigma_{\text{off}}^2 \rfloor), \quad (22)$$

where $\lfloor \cdot \rfloor$ is the largest integer that is not greater than the argument. Then, we draw $N \times L^{\text{HQS}}$ variables, denoted by $x_{i\ell}$ (with $i \in \{1, \dots, N\}$ and $\ell \in \{1, \dots, L^{\text{HQS}}\}$), independently from the identical normal distribution with mean $\sqrt{\mu_{\text{off}}/L^{\text{HQS}}}$ and variance $-\mu_{\text{off}}/L^{\text{HQS}} + \sqrt{\mu_{\text{off}}^2/(L^{\text{HQS}})^2 + \sigma_{\text{off}}^2/L^{\text{HQS}}}$. Then, the H-Q-S algorithm sets the covariance matrix by

$$C_{ij}^{\text{HQS}} = \sum_{\ell=1}^{L^{\text{HQS}}} x_{i\ell} x_{j\ell} \quad i, j \in \{1, \dots, N\}. \quad (23)$$

It is known that $\langle C^{\text{HQS}} \rangle_{ij} = \delta_{ij} \mu_{\text{on}} + (1 - \delta_{ij}) \mu_{\text{off}}$. Therefore, the expectation of the correlation matrix, ρ^{HQS} , is approximately given by $\langle \rho^{\text{HQS}} \rangle_{ij} = \delta_{ij} + (1 - \delta_{ij}) \mu_{\text{off}} / \mu_{\text{on}}$. The degree of correlation networks is usually heterogeneously distributed. This property is not captured by the H-Q-S algorithm [224].

A configuration model for covariance matrices that preserves the expectation of each row sum excluding the diagonal entry, which is equivalent to each node's degree in the case of the adjacency matrix of a conventional network, can be defined as follows [218]. This algorithm, which we refer to as the correlation matrix configuration model, preserves the expectation of each diagonal entry of C^{sam} , or the variance of each variable, and the expectation of each row sum excluding the diagonal entry, i.e., $\sum_{j=1; j \neq i}^N C_{ij}^{\text{sam}} \forall i$, corresponding to the degree of the i th node. Under these constraints, the correlation matrix configuration model uses the distribution of $x_{i\ell}$, determined from the maximum entropy principle. In fact, each $(x_{1\ell}, \dots, x_{N\ell})^\top$, $\ell \in \{1, \dots, L\}$, independently obeys an identical multivariate normal distribution whose mean is the zero matrix and covariance matrix is denoted by C^{cm} . Therefore, the correlation matrix configuration model is the Wishart distribution $W_N(C^{\text{cm}}, L)$. Matrix C^{cm} is of the form $[(C^{\text{cm}})^{-1}]_{ij} = -[\delta_{ij} \cdot 2\alpha_i + (1 - \delta_{ij})(\beta_i + \beta_j)]$, where α_i and β_i are parameters to be determined. One determines the values of α_i and β_i using a gradient descent algorithm [218] or by reformulating the problem as a convex optimization problem and solving it [186].

4 Network-analysis inspired analysis directly applied to correlation matrices

As we already mentioned, a straightforward way to use null models for correlation matrices as controls of correlation networks is to generate correlation networks from the correlation matrix generated by the null model or its distribution. In this section, we showcase another usage of null models for correlation matrices, which is to conduct analysis inspired by network analysis but directly on correlation matrix data with the help of null model correlation matrices. Crucially, this scenario does not involve transformation of a given correlation matrix into a correlation network. To

explain the idea, consider financial time series analysis using correlation matrices. Portfolio optimization and random matrix theory directly applied to correlation matrix data are among powerful techniques to analyze such data [6]. These methods do not suffer from difficulties in transforming correlation matrices into correlation networks because they do not carry out such a transformation. In contrast, a motivation behind carrying out such a transformation is that one can then use various network analysis methods. A strategy to take advantage of both approaches is to adapt network analysis methods for conventional networks to the case of correlation matrix data.

4.1 Degree

Many empirical networks show heterogeneous degree distributions such as a power-law-like distribution [217, 225]; such networks are called scale-free networks. The same holds true for the weighted degree of many networks [226]. Correlation networks are no exception, not much depending on how one constructs a network from correlation matrix data [194, 218, 227–229].

If we do not transform the given correlation matrix into a network, the node’s weighted degree represents how the node’s signal, X_i , is close to the signal averaged over all the nodes, X_{total} , as shown in Eq. (13). Previous research showed that the weighted degree calculated in this manner is heterogeneously distributed for some empirical data, while the right tail of the distribution is not as fat as typical degree distributions for conventional empirical networks [218]. The results are qualitatively similar when one calculates the weighted degree of the i th node as $\sum_{j=1; j \neq i}^N |C_{ij}|$ or $\sum_{j=1; j \neq i; C_{ij} > 0}^N C_{ij}$. Therefore, heterogeneous degree distributions of the correlation network are not an artifact of the thresholding or other operations for creating networks from correlation data, at least to some extent.

4.2 Community detection

Community structure in networks is a partition of the nodes into (generally non-overlapping) groups that are internally well connected and sparsely connected across. One can detect communities with many different algorithms, and one popular family of methods, despite some shortcomings [128], is modularity maximization [210, 230], which aims at placing a higher-than-expected number of edges connecting nodes within the same community. Modularity with a resolution parameter γ is defined by

$$Q = \frac{1}{N\bar{k}} \sum_{i,j=1}^N \left(A_{ij} - \gamma \frac{k_i k_j}{N\bar{k}} \right) \delta_{g_i, g_j}, \quad (24)$$

where we remind that A_{ij} is the entry of the empirical adjacency matrix, g_i is the community in which the i th node is placed by the current partition, and δ is again the Kronecker delta. Note the presence of the term $k_i k_j / N\bar{k}$ coming from Eq. (12), which signifies the use of the configuration model as standard null model in the ordinary modularity for networks. Approximate maximization of Q by varying g_1, \dots, g_N for a given network identifies its community structure.

Community detection, in particular modularity maximization, is desirable for correlation network data, too. Given that the original correlation matrix has both positive and negative entries in general, a possible variant of modularity maximization for correlation networks is to maximize a modularity designed for signed networks. The modularity for signed networks may be defined as a weighted difference of the modularity calculated for the positive network (i.e., the weighted network only containing positively weighted edges) and the modularity calculated for the negative network (i.e., the weighted network only containing negatively weighted edges with the edge weight being the absolute value of the correlation) [123]. However, this procedure assumes that, in the null model, edges can be thought as independent (as in the model described by Eq. (12)) and that positive edges can be randomized independently of negative edges. We have seen that both assumptions are clearly not valid for correlation matrices.

One can bypass the analogy with networks by directly computing and maximizing a modularity function that is appropriately defined for correlation matrices [90]. A viable redefinition of modularity for correlation matrices is given by

$$Q^{\text{cor}} = \frac{1}{\mathcal{N}} \sum_{i,j=1}^N (\rho_{ij}^{\text{sam}} - \langle \rho_{ij} \rangle) \delta_{g_i, g_j}, \quad (25)$$

where $\mathcal{N} = \sum_{i,j=1}^N \rho_{ij}^{\text{sam}}$ is a normalization constant. Matrix $\langle \rho \rangle$ is a proper null model for the correlation matrix, which one can scale by a resolution parameter γ if desired. Approximate maximization of Q^{cor} provides communities in correlation matrices. The crucial ingredient is the choice of the null model, $\langle \rho_{ij} \rangle$. Depending on what features of the original data one desires to preserve, the use of any of the models described in section 3.8 is in principle

legitimate, e.g., the white-noise (identity matrix) model $\rho_{ij}^{\text{MG1}} = \delta_{ij}$, the noise-only model ρ_{ij}^{MG2} , the noise+global model ρ_{ij}^{MG3} , or the correlation matrix configuration model C_{ij}^{cm} . However, note that in the summation in Eq. (25) some terms must be positive and some must be negative in order to identify a nontrivial community structure, i.e., one different from a single community enclosing all nodes. For example, if all the entries of the empirical correlation matrix, ρ^{sam} , are positive, then the null model ρ^{MG1} will keep all terms in the summation in Eq. (25) non-negative, and the resulting optimal partition will be a single community [90]. By contrast, the use of ρ^{MG2} yields negative terms in the same situation unless a global trend is present. If a global trend is present, one obtains the best results by using ρ^{MG3} , which reveals group-specific correlations [90]. Modularity maximization using ρ^{MG3} has successfully revealed nontrivial community structure in time series of financial stock prices [90–92], credit default swaps [93], brain rhythms [231], and in single-cell gene expression profiles [66].

4.3 Clustering coefficient

Clustering coefficients measure the abundance of triangles in a network [217]. A dominant definition of clustering coefficient for unweighted networks, denoted by \tilde{C} , is given by [206]

$$\tilde{C} = \frac{1}{N} \sum_{i=1}^N \tilde{C}_i, \quad (26)$$

where \tilde{C}_i is the local clustering coefficient at the i th node given by

$$\tilde{C}_i = \frac{(\text{number of triangles involving the } i\text{th node})}{k_i(k_i - 1)/2}. \quad (27)$$

The denominator of the right-hand side of Eq. (27) is a normalization constant to ensure that $0 \leq \tilde{C}_i \leq 1$.

One often measures clustering coefficients for both unweighted and weighted correlation networks. There are various definitions of weighted clustering coefficients [232,233]. One definition [228] is given by $\tilde{C}_i^{\text{wei,Z}} = N^{-1} \sum_{i=1}^N \tilde{C}_i^{\text{wei,Z}}$, where

$$\tilde{C}_i^{\text{wei,Z}} = \frac{1}{\max_{i'j'} w_{i'j'}} \frac{\sum_{\substack{1 \leq j, \ell \leq N \\ j, \ell \neq i}} w_{ij} w_{i\ell} w_{j\ell}}{\sum_{\substack{1 \leq j, \ell \leq N \\ j, \ell \neq i; j \neq \ell}} w_{ij} w_{i\ell}}, \quad (28)$$

and w_{ij} ($= w_{ji} \geq 0$) is the weight of edge (i, j) .

Many empirical networks show large unweighted or weighted clustering coefficient values, and correlation networks are no exception. However, as we pointed out in section 3.2, a high clustering coefficient of the correlation network is at least partly due to pseudo correlation.

Given this background, clustering coefficients for correlation matrices were proposed using a similar idea to the case of modularity directly defined for correlation matrices [234]. Because correlation matrices are naturally clustered if we threshold on the Pearson correlation matrix, the authors used the three-way partial correlation coefficient or partial mutual information to partial out the effect of a common neighbor of nodes j and ℓ (say i) to quantify partial connection between j and ℓ . In other words, we measure the connectivity between neighbors of i by, for example, the partial correlation coefficient $\rho(X_j, X_\ell | X_i)$, which we abbreviate as $\rho_{j\ell|i}$; the partial correlation coefficient is defined by Eq. (16). Because there is no clear notion of neighborhood for correlation matrices, we need to consider all triplets of different nodes, (i, j, ℓ) . Then, as for the definition of the original clustering coefficient for networks, they took the average of $\rho_{j\ell|i}$ over the i th node's neighbors j and ℓ to define a local clustering coefficient for i . For example, we define a local clustering coefficient for node i as a weighted average by

$$C_i^{\text{cor,A}} = \frac{\sum_{\substack{1 \leq j < \ell \leq N \\ j, \ell \neq i}} |\rho_{ij} \rho_{i\ell} \rho_{j\ell|i}|}{\sum_{\substack{1 \leq j < \ell \leq N \\ j, \ell \neq i}} |\rho_{ij} \rho_{i\ell}|}. \quad (29)$$

Finally, as in the case of the clustering coefficient for networks, we define the global clustering coefficient by $C^{\text{cor,A}} = \sum_{i=1}^N C_i^{\text{cor,A}}/N$. This method borrows the idea of clustering coefficient from complex network studies and tailors it for correlation matrix data. Clustering coefficients $C_i^{\text{cor,A}}$ and $C^{\text{cor,A}}$ already partial out the effect of pseudo correlation between X_j and X_ℓ due to X_i . However, we can still compare the observed clustering coefficient values against those for null models to validate whether or not the clustering coefficient values for the given data are significantly different from those for the null model [218].

5 Software

In this section, we introduce freely available code useful for analyzing correlation networks. Obviously, one can apply software for analyzing general unweighted or weighted networks after thresholding (and optionally further dichotomizing) the given correlation matrix data. There are numerous packages for unweighted and weighted network analysis, which we do not mention here without a few exceptions.

In gene correlation network analysis, Weighted Correlation Network Analysis (WGCNA) is a popular freely available R software package [60]. WGCNA provides various outputs, such as community structure, weighted clustering coefficients, and visualization. WGCNA transforms the original edge weight, denoted by w_{ij} for edge (i, j) , by a so-called soft thresholding transformation, i.e., by $|w_{ij}|^\beta$, where $\beta \geq 1$ is a parameter³, such that one obtains an unsigned weighted network. Phiclust [66] is another community-detection tool for correlations from single-cell gene expression data, derived from random matrix theory (i.e., Wishart ensemble as described in section 3.8). It can be used to identify cell clusters with non-random substructure, possibly leading to the discovery of previously overlooked phenotypes. Phiclust is written in R and is freely available at Github [235] and Zenodo under GNU General Public License V3.0 [236].

The Brain Connectivity Toolbox is a MATLAB toolbox for analyzing networks [237]. It is also implemented in Python. Despite the name, many of the functions provided by the Brain Connectivity Toolbox can be applied to general network data, and many people outside neuroscience also use it. In relation to correlation networks, this toolbox is particularly good at handling weighted and signed networks, such as their degree, clustering coefficients, and community structure.

The graph-tool module in Python provides powerful network analysis and visualization functionality [238]. In relation to correlation networks, graph-tool is particularly strong at network inference based on stochastic block models.

The bootnet package in R can be used for estimating psychological networks using graphical lasso, with a unique feature of being able to assess the accuracy of the estimated network [38]. This package can be used for other types of correlation matrix data as well. Also see [38, 239] for various R packages for sparse and related estimation of the precision and covariance matrices. For example, the qgraph package can also generate networks using the graphical lasso and visualize Pearson and partial correlation matrices [240], with beginner-friendly tutorials (e.g., [241]).

Graphical lasso is also implemented in Python, through the GraphicalLassoCV function in the scikit-learn package [242, 243]. The sklearn.covariance package also contains other functions for covariance estimation such as covariance shrinkage. Table 2 of [18] lists other code packages for estimating graphical models as well as different models.

Papers [90, 208] contain references to Python, MATLAB, and R codes for generating null models of correlation matrices discussed in section 3.8. For example, the “spatiotemporal modeling tools for Python” contains functions to generate null model correlation matrices such as the H-Q-S model (named Zalesky matching model in their package) and methods through generating surrogate time series [222]. Another package in the list is the Scola, in Python, which generates the H-Q-S model and the correlation matrix configuration model [186]. Finally, a MATLAB package on MathWorks [244] implements the null models based on random matrix theory, $\rho^{\text{MG}2}$ and $\rho^{\text{MG}3}$, derived in [90] from the Wishart ensemble.

6 Outlook

We have reviewed various techniques to obtain and analyze networks generated from correlation matrix data, which naturally arise across many domains. Sections 2 and 3 emphasize for readers that there is not a single dominant method. We also highlighted good practices and pitfalls of individual methods. Naïve applications of network generation and analysis methods to correlation matrix data can easily yield flawed results. We should be careful about both how to generate correlation networks and how to analyze them. Specifically, in resonance with previous reports, we explained that a simplistic dichotomizing, which is widely used, is problematic for multiple reasons (see section 3.2). The problems, i.e., lack of an established method to set the threshold value, false positives, and losing the values of subthreshold correlation values, are shared by weighted networks generated by thresholding (without dichotomizing). Our recommendation is to resort to other methods, such as partial correlation networks, graphical lasso (which is a partial correlation network method) and its variants, and covariance shrinkage, which avoid some of these problems. Another option is to still use the simplistic thresholding, possibly followed by dichotomization, but combine it with a proper null model to avoid pitfalls. Although thresholded correlation networks have high

³The soft thresholding here, coined in [60], is different from the same term defined in section 3.3. It also does not belong to thresholding in the sense used in this article (defined in section 3.2).

clustering no matter what data we use, a proper null model (e.g., shuffling of $\{x_{i\ell}\}$) will also produce thresholded correlation networks with high clustering. Therefore, by comparing the results with those for the null model, one can avoid wrong conclusions such as that almost all empirical correlation networks have high clustering. We recall that null models for networks, most famously the configuration model, are not a proper null model for correlation networks because they generally do not originate from correlation matrices and do not generally match key properties of typical correlation matrices. See section 3.8 for proper choices. We conclude this article by stating some promising directions for future research.

Reproducibility of correlation networks arising from common approaches is a major practical issue, as has been pointed out in the literature in psychology and psychotherapy (e.g. [42, 48]) and microbiome analysis [79]. In these research fields and others, it is often the case that only relatively few samples are available given the size of matrix and network, N , we wish to analyze. Especially if the number of samples, L , is smaller than or close to N , the partial correlation matrix and spectra of random matrices carry large variation, in part because they are inherently rank deficient. From the statistical inference point of view, it is not sound to try to infer many parameters, such as entries of the covariance matrix, from relatively few observations. The recognition of such phenomena led to the idea of covariance selection and various other methods. The amount of data needed for reliably estimating correlation networks, i.e., power analysis in statistics, should be further pursued for various correlation matrix data [38]. The development of methods to help practitioners use correlation networks better (e.g., by providing uncertainty quantification or clarifying the various noise trade-offs) can be transformational. Despite these challenges, there is a pressing need to understand complex systems of a very high dimension (i.e., $N \gg L$) with correlational data. One approach to this problem is to formulate estimation of large correlation networks as a computational rather than statistical challenge, as a problem to be solved under runtime and memory constraints, and to search feasible solutions in combination with machine learning [1]. How to reconcile the statistical and computational types of approach and deepen usage of machine learning and artificial intelligence techniques to correlation network analysis may be a beneficial research direction.

A key outstanding question is the treatment of low-correlation edges. On one hand, we have surveyed attempts to remove “noise” edges (for example by thresholding or graphical lasso), which is supposed to improve the overall signal-to-noise ratio of the graph representation. Sparser models are more parsimonious, easier to process quickly and with a lower memory footprint, and amenable to a range of network science analysis tools. On the other hand, one can argue that getting rid of low-correlation edges risks losing valuable information (see section 3.2). In fact, it has been shown in the neuroscience context that the low-correlation edges alone can have substantial predictive power [143, 245, 246].

A related question is how to use *a priori* domain knowledge to choose appropriate preprocessing steps, such as what threshold to apply and whether or not to dichotomize. For example, dichotomizing may be more appropriate when the *a priori* belief is that nodes are either coordinating or not, with no appreciable difference in the degree of coordination when two nodes coordinate. As another example, one could use random matrix theory on domain-relevant distributions to compare the dominant eigenvectors or eigenvalues before and after thresholding. This exercise may provide guidance on when thresholding is unlikely to have adverse effects.

Another viable alternative to the current focus on trying to recover and analyze the most accurate possible correlation matrix may be to treat the constructed correlation network as inherently uncertain and to regard it as a sample from a distribution of possible matrices as part of the analysis. For example, when assessing community structure, it may make sense to focus on structures that appear consistently across samples of correlation networks drawn from the estimated distribution, even when exact correlation values (perhaps especially the weaker correlations) considerably vary from sample to sample. Although there are established ways to do this for general networks [247], we are not aware of any work either applying these approaches to correlation networks or developing theory and methods tailored to correlation networks. Such approaches may leverage existing work on null models for correlation networks, for example, as priors when forming a posterior distribution to sample from. On the other hand, some studies have documented the stability of the detected correlation-induced communities across time and their robustness under change of temporal resolution [90, 93].

There are many multilayer network data sets, including multilayer correlation matrix data sets, and various data-analysis methods for them [190, 248–250]. Examples include brain activity, where different layers of correlation matrices correspond to, for example, different frequency bands [251–254], or brain activity during different tasks [255]. In gene co-expression networks, different layers correspond to, for example, different levels of co-expression between gene pairs [256] or different tissue types such as different organs [257]. Overlaying different methods to construct correlation networks from one data set in each layer is another method to construct multilayer correlation matrices [258]. There are methods for analyzing multilayer correlation matrices and networks such as multilayer community detection algorithms [190, 257]. However, methods that exploit the mathematical nature of correlation matrices data are still scarce and left for future work. Furthermore, multilayer networks are a major representation

of temporal network data, where each layer corresponds to one time window [187, 190, 259]. Therefore, methods for analyzing multilayer correlation network data will also contribute to analysis of time-varying correlation network data.

Similar to other studies, we emphasize the potentially negative effects of thresholding, motivating our explanation of other methods for constructing correlation networks. However, thresholding also has positive effects such as reducing false positives by discarding edges with small weights including the case of correlation networks. Such positive effects of thresholding may be manifested in multilayer data. For example, aggregating layers in a multilayer network and dichotomizing the aggregated edge weight can enhance detectability of multilayer communities compared to no thresholding under certain conditions [260, 261]. Furthermore, some layers in a multilayer network may be more informative than other layers. While these arguments are for general multilayer networks, many of them may directly apply to multilayer correlation matrices.

In section 4, we showcased some methods for analyzing correlation matrix data without transforming them into correlation networks but yet by benefiting from ideas and formulations of network analysis. Although we only presented the degree, modularity maximization and clustering coefficients, this approach is generalizable to other structural properties and analysis methods formulated for networks. Examples include various node centrality measures, motifs, community detection methods apart from modularity maximization, rich clubs, fractals, and simplicial complexes.

For a given N , the set of covariance matrices constitutes the positive semidefinite cone, which is convex. Similarly, the set of full-rank correlation matrices, which is a strict subset of full-rank covariance matrices, is called the elliptope [121, 122]. Positive semidefinite cones and elliptopes are manifolds and have their own geometric structure, which have been suggested to be useful for measuring the similarity between pairs of covariance or correlation matrices. Quantitative comparison of two covariance and correlation matrices is useful for various tasks such as fingerprinting of individuals, anomaly detection, and change-point detection in multivariate time series data. A straightforward way to measure the distance between two covariance/correlation matrices is to use a common matrix

norm such as the Frobenius norm (i.e., $\sqrt{\sum_{i=1}^N \sum_{j=1}^N |\rho_{ij}^{(1)} - \rho_{ij}^{(2)}|^2}$ in the case of correlation matrices, where $\rho^{(1)}$ and $\rho^{(2)}$ are two correlation matrices). However, research (in particular in neuroimaging studies) has suggested that geodesic distance measures respecting the structure of these manifolds is better at, for example, fingerprinting of individuals from fMRI data [262–264]. In these geodesic distance measures, one considers the tangent space at a given point x on the manifold, which corresponds to a correlation/covariance matrix. The so-called exponential map provides a one-to-one mapping from the straight line segment on the tangent space, which is essentially the Euclidean space, to the geodesic from x to y on the manifold. The logarithm map is the inverse of the exponential map. The geodesic distance between x and y is the length of the geodesic and has a practical matrix algebraic formula. Multiple reasonable definitions of such geodesic distances exist [263]. See [263, 265, 266] for mathematical expositions. Although these techniques are not for correlation networks but for matrices, they may potentially benefit understanding and algorithms for correlation networks. For example, can we understand null models of correlation matrices as a projection onto a submanifold of the entire elliptope? What are geometric meanings of thresholding, dichotomizing, and other operations to create correlation networks? Do we benefit by measuring distances between correlation networks rather than between correlation matrices?

One complication that has not received enough attention is that many in-practice comparisons involve ensembles of observed networks rather than single networks. This is the case in most fMRI studies where networks are used. When working with an ensemble of networks, one must make various decisions, such as whether or not to ensure that edge density is constant across networks (see section 3.2 for the absolute versus proportional threshold). The development of mathematical theories for how to construct correlation-based networks for ensembles may be helpful because most null models and other tools are only oriented toward single networks. Multilayer approach and geometric approaches to correlation networks and matrices, both of which cater to between-network/matrix comparisons, are promising paths towards this goal.

A graphon is a symmetric measurable function $W : [0, 1]^2 \rightarrow [0, 1]$. Given W , we generate dense graphs in which there is an edge between the i th and j th nodes with probability $W(u_i, u_j)$, where each $u_i \forall i$ independently obeys the uniform density on $[0, 1]$ [267]. In network science, assigning a node weight, either from a probability distribution or empirical data, and connecting two nodes probabilistically as a function of the two node weights has been a major method to generate networks [268–274]. Basic correlation networks are equivalent to an extension of this class of network models where u_i is an L -dimensional vector of the i th feature from L samples, and W is a criterion with which to determine the edge. In fact, similar to the construction of correlation networks by dichotomizing, dichotomizing functions have been used as W to generate networks with power-law degree distributions from scalar node weights that do not have to obey long-tailed distributions [271, 273, 275–277]. Importing mathematical frameworks and methods from graphon-related models, such as the limit of a sequence of dense networks, to correlation network

analysis may be an interesting idea. Those frameworks may be able to provide null models for correlation networks or give more mathematical foundations of correlation networks.

We have seen that there are various research fields in which they collect and analyze correlation networks. We have also seen that some particular analysis techniques are heavily studied in one field, but others are preferred in different fields. For example, random matrices for correlation matrices have particularly been used in financial data studies, including econophysics. As another example, a majority of studies of temporal correlation networks has been done in network neuroscience under the name of dynamic functional connectivity/networks. However, very often, methods for analyzing correlation networks developed in one research field do not rely on particularities of the field and are therefore transferable to other research fields. While such cross-fertilization has been ongoing and advocated [18], we emphasize that much more of it will be useful for furthering correlation network analysis and applications.

Acknowledgements

N.M. acknowledges support from National Institute of General Medical Sciences (under grant no. R01GM148973), the Japan Science and Technology Agency (JST) Moonshot R&D (under grant no. JPMJMS2021), the National Science Foundation (under grant nos. 2052720 and 2204936), and JSPS KAKENHI (under grant nos. JP 21H04595 and 23H03414). P.J.M. and Z.M.B. acknowledge support from the Army Research Office (under MURI award W911NF-18-1-0244). P.J.M. also acknowledges support from the National Institute of Diabetes and Digestive and Kidney Diseases (under grant no. R01DK125860) and from the National Science Foundation (under grant no. 2140024). Z.M.B. also acknowledges support from the National Science Foundation (under grant no. 2137511). D.G. acknowledges support by the European Union - NextGenerationEU - National Recovery and Resilience Plan (Piano Nazionale di Ripresa e Resilienza, PNRR), project ‘SoBigData.it - Strengthening the Italian RI for Social Mining and Big Data Analytics’ - Grant IR0000013 (n. 3264, 28/12/2021) (<https://pnrr.sobigdata.it/>). The content is solely the responsibility of the authors and does not necessarily represent the official views of any agency supporting this work.

References

- [1] M. Becker, H. Nassar, C. Espinosa, I. A. Stelzer, D. Feyaerts, E. Berson, Neda H. Bidoki, A. L. Chang, G. Saaranya, A. Culos, D. De Francesco, R. Fallahzadeh, Q. Liu, Y. Kim, I. Marić, S. J. Mataraso, S. N. Payrovnaziri, T. Phongpreecha, N. G. Ravindra, N. Stanley, S. Shome, Y. Tan, M. Thuraiappah, M. Xenochristou, L. Xue, G. Shaw, D. Stevenson, M. S. Angst, B. Gaudilliere, and N. Aghaeepour. Large-scale correlation network construction for unraveling the coordination of complex biological systems. *Nat. Comput. Sci.*, 3:346–359, 2023.
- [2] I. T. Jolliffe. *Principal Component Analysis*. Springer, New York, NY, second edition, 2002.
- [3] T. W. Anderson. *An Introduction to Multivariate Statistical Analysis*. John Wiley & Sons, Hoboken, NJ, third edition, 2003.
- [4] S. A. Mulaik. *Foundations of Factor Analysis*. Taylor & Francis, Boca Raton, FL, second edition, 2010.
- [5] H. Markowitz. Portfolio selection. *J. Finance*, 7:77–91, 1952.
- [6] J. Bun, J. P. Bouchaud, and M. Potters. Cleaning large correlation matrices: Tools from Random Matrix Theory. *Phys. Rep.*, 666:1–109, 2017.
- [7] B. Podobnik and H. E. Stanley. Detrended cross-correlation analysis: A new method for analyzing two non-stationary time series. *Phys. Rev. Lett.*, 100:084102, 2008.
- [8] X.-Y. Qian, Y.-M. Liu, Z.-Q. Jiang, B. Podobnik, W.-X. Zhou, and H. E. Stanley. Detrended partial cross-correlation analysis of two nonstationary time series influenced by common external forces. *Phys. Rev. E*, 91:062816, 2015.
- [9] N. Yuan, Z. Fu, H. Zhang, L. Piao, E. Xoplaki, and J. Luterbacher. Detrended partial-cross-correlation analysis: A new method for analyzing correlations in complex system. *Sci. Rep.*, 5:8143, 2015.
- [10] D. Y. Kenett, M. Tumminello, A. Madi, G. Gur-Gershoren, R. N. Mantegna, and E. Ben-Jacob. Dominating clasp of the financial sector revealed by partial correlation analysis of the stock market. *PLoS ONE*, 5:e15032, 2010.

- [11] D. Y. Kenett, T. Preis, G. Gur-Gershgoren, and E. Ben-Jacob. Dependency network and node influence: Application to the study of financial markets. *Int. J. Bifu. Chaos*, 22:1250181, 2012.
- [12] D. Zhou, A. Gozolchiani, Y. Ashkenazy, and S. Havlin. Teleconnection paths via climate network direct link detection. *Phys. Rev. Lett.*, 115:268501, 2015.
- [13] L. Chen, R. Liu, Z.-P. Liu, M. Li, and K. Aihara. Detecting early-warning signals for sudden deterioration of complex diseases by dynamical network biomarkers. *Sci. Rep.*, 2:342, 2012.
- [14] S. Chen, E. B. O’Dea, J. M. Drake, and B. I. Epureanu. Eigenvalues of the covariance matrix as early warning signals for critical transitions in ecological systems. *Sci. Rep.*, 9:2572, 2019.
- [15] N. G. MacLaren, P. Kundu, and N. Masuda. Early warnings for multi-stage transitions in dynamics on networks. *J. R. Soc. Interface*, 20:20220743, 2023.
- [16] T. Watanabe, N. Masuda, F. Megumi, R. Kanai, and G. Rees. Energy landscape and dynamics of brain activity during human bistable perception. *Nat. Comm.*, 5:4765, 2014.
- [17] T. Ezaki, T. Watanabe, M. Ohzeki, and N. Masuda. Energy landscape analysis of neuroimaging data. *Phil. Trans. R. Soc. A*, 375:20160287, 2017.
- [18] D. Borsboom, M. K. Deserno, M. Rhemtulla, S. Epskamp, E. I. Fried, R. J. McNally, D. J. Robinaugh, M. Perugini, J. Dalege, G. Costantini, A.-M. Isvoranu, A. C. Wysocki, C. D. van Borkulo, R. van Bork, and L. J. Waldorp. Network analysis of multivariate data in psychological science. *Nat. Rev. Methods Primers*, 1:58, 2021.
- [19] X. Liu, Y. Liu, J. Chen, and X. Liu. PSCC-Net: Progressive spatio-channel correlation network for image manipulation detection and localization. *IEEE Trans. Circ. Syst. Video Technol.*, 32:7505–7517, 2022.
- [20] M. Lee, C. Park, S. Cho, and S. Lee. Superpixel group-correlation network for co-saliency detection. In *Proceedings of the International Conference on Image Processing (ICIP)*, pages 806–810, 2022.
- [21] Z. Tu, Z. Li, C. Li, and J. Tang. Weakly alignment-free RGBT salient object detection with deep correlation network. *IEEE Trans. Image Proc.*, 31:3752–3764, 2022.
- [22] U. von Luxburg. A tutorial on spectral clustering. *Stat. Comput.*, 17:395–416, 2007.
- [23] M. Tumminello, C. Coronello, F. Lillo, S. Micciche, and R. N. Mantegna. Spanning trees and bootstrap reliability estimation in correlation-based networks. *Int. J. Bifu. Chaos*, 17:2319–2329, 2007.
- [24] M. Tumminello, F. Lillo, and R. N. Mantegna. Correlation, hierarchies, and networks in financial markets. *J. Econ. Behav. Org.*, 75:40–58, 2010.
- [25] S. M. Smith, K. L. Miller, G. Salimi-Khorshidi, M. Webster, C. F. Beckmann, T. E. Nichols, J. D. Ramsey, and M. W. Woolrich. Network modelling methods for fMRI. *NeuroImage*, 54:875–891, 2011.
- [26] K. Faust and J. Raes. Microbial interactions: From networks to models. *Nat. Rev. Microbiol.*, 10:538–550, 2012.
- [27] F. De Vico Fallani, J. Richiardi, M. Chavez, and S. Achard. Graph analysis of functional brain networks: Practical issues in translational neuroscience. *Phil. Trans. R. Soc. B*, 369:20130521, 2014.
- [28] Y. X. R. Wang and H. Huang. Review on statistical methods for gene network reconstruction using expression data. *J. Theor. Biol.*, 362:53–61, 2014.
- [29] A. Fukushima, M. Kusano, H. Redestig, M. Arita, and K. Saito. Metabolomic correlation-network modules in *Arabidopsis* based on a graph-clustering approach. *BMC Syst. Biol.*, 5:1, 2011.
- [30] T. Millington and M. Niranjan. Construction of minimum spanning trees from financial returns using rank correlation. *Physica A*, 566:125605, 2021.
- [31] A. J. Butte and I. S. Kohane. Mutual information relevance networks: Functional genomic clustering using pairwise entropy measurements. In *Pacific Symposium on Biocomputing*, pages 418–429, Singapore, 2000. World Scientific.

- [32] P. E. Meyer, F. Lafitte, and G. Bontempi. minet: A r/bioconductor package for inferring large transcriptional networks using mutual information. *BMC Bioinformatics*, 9:461, 2008.
- [33] X. Guo, H. Zhang, and T. Tian. Development of stock correlation networks using mutual information and financial big data. *PLoS ONE*, 13:e0195941, 2018.
- [34] R. Salvador, J. Suckling, C. Schwarzbauer, and E. Bullmore. Undirected graphs of frequency-dependent functional connectivity in whole brain networks. *Phil. Trans. R. Soc. B*, 360:937–946, 2005.
- [35] P. Fiedor. Partial mutual information analysis of financial networks. *Acta Physica Polonica A*, 127:863–867, 2015.
- [36] J. Pearl. Causal inference. *Journal of Machine Learning Research Workshop and Conference Proceedings*, 6:39–58, 2010.
- [37] J. Runge, S. Bathiany, E. Bollt, G. Camps-Valls, D. Coumou, E. Deyle, C. Glymour, M. Kretschmer, M. D. Mahecha, J. Muñoz-Marí, E. H. van Nes, J. Peters, R. Quax, M. Reichstein, M. Scheffer, B. Schölkopf, P. Spirtes, G. Sugihara, J. Sun, K. Zhang, and J. Zscheischler. Inferring causation from time series in Earth system sciences. *Nat. Commun.*, 10:2553, 2019.
- [38] S. Epskamp, D. Borsboom, and E. I. Fried. Estimating psychological networks and their accuracy: A tutorial paper. *Behav. Res.*, 50:195–212, 2018.
- [39] G. M. Harari, N. D. Lane, R. Wang, B. S. Crosier, A. T. Campbell, and S. D. Gosling. Using smartphones to collect behavioral data in psychological science: Opportunities, practical considerations, and challenges. *Perspectives on Psychological Science*, 11:838–854, 2016.
- [40] A. L. McGowan, F. Sayed, Z. M. Boyd, M. Jovanova, Y. Kang, M. E. Speer, D. Cosme, P. J. Mucha, K. N. Ochsner, D. S. Bassett, E. B. Falk, and D. M. Lydon-Staley. Dense sampling approaches for psychiatry research: Combining scanners and smartphones. *Biol. Psychiatry*, 93:681–689, 2023.
- [41] D. Borsboom and A. O. J. Cramer. Network analysis: An integrative approach to the structure of psychopathology. *Annu. Rev. Clin. Psychol.*, 9:91–121, 2013.
- [42] E. I. Fried and A. O. J. Cramer. Moving forward: Challenges and directions for psychopathological network theory and methodology. *Pers. Psychol. Sci.*, 12:999–1020, 2017.
- [43] E. I. Fried, C. D. van Borkulo, A. O. J. Cramer, L. Boschloo, R. A. Schoevers, and D. Borsboom. Mental disorders as networks of problems: A review of recent insights. *Soc. Psychiatry Psychiatr. Epidemiol.*, 52:1–10, 2017.
- [44] A. L. McGowan, Z. M. Boyd, Y. Kang, L. Bennett, P. J. Mucha, K. N. Ochsner, D. S. Bassett, E. B. Falk, and D. M. Lydon-Staley. Within-person temporal associations among self-reported physical activity, sleep, and well-being in college students. *Psychosomatic Medicine*, 85:141–153, 2023.
- [45] S. Epskamp, L. J. Waldorp, R. Möttus, and D. Borsboom. The Gaussian graphical model in cross-sectional and time-series data. *Multivar. Behav. Res.*, 53:453–480, 2018.
- [46] W. Lutz, B. Schwartz, S. G. Hofmann, A. J. Fisher, K. Husen, and J. A. Rubel. Using network analysis for the prediction of treatment dropout in patients with mood and anxiety disorders: A methodological proof-of-concept study. *Sci. Rep.*, 8:7819, 2018.
- [47] D. C. R. van Zelst, E. M. Veltman, D. Rhebergen, P. Naarding, A. A. L. Kok, N. R. Ottenheim, and E. J. Giltay. Network structure of time-varying depressive symptoms through dynamic time warp analysis in late-life depression. *Int. J. Geriatr. Psychiatry*, 37:1–12, 2022.
- [48] M. K. Forbes, A. G. C. Wright, K. E. Markon, and R. F. Krueger. Evidence that psychopathology symptom networks have limited replicability. *J. Abnormal Psychol.*, 126:969–988, 2017.
- [49] E. Bullmore and O. Sporns. Complex brain networks: Graph theoretical analysis of structural and functional systems. *Nat. Rev. Neurosci.*, 10:186–198, 2009.
- [50] D. S. Bassett and O. Sporns. Network neuroscience. *Nat. Neurosci.*, 20:353–364, 2017.

- [51] J. Chung, E. Bridgeford, J. Arroyo, B. D. Pedigo, A. Saad-Eldin, V. Gopalakrishnan, L. Xiang, C. E. Priebe, and J. T. Vogelstein. Statistical connectomics. *Annu. Rev. Stat. Appl.*, 8:463–492, 2021.
- [52] R. C. Craddock, S. Jbabdi, C.-G. Yan, J. T. Vogelstein, F. X. Castellanos, A. Di Martino, C. Kelly, K. Heberlein, S. Colcombe, and M. P. Milham. Imaging human connectomes at the macroscale. *Nat. Methods*, 10:524–539, 2013.
- [53] B. Biswal, F. Z. Yetkin, V. M. Haughton, and J. S. Hyde. Functional connectivity in the motor cortex of resting human brain using echo-planar MRI. *Magnetic Resonance in Medicine*, 34:537–541, 1995.
- [54] G. L. Colclough, M. W. Woolrich, P. K. Tewarie, M. J. Brookes, A. J. Quinn, and S. M. Smith. How reliable are MEG resting-state connectivity metrics? *NeuroImage*, 138:284–293, 2016.
- [55] A. Alexander-Bloch, J. N. Giedd, and E. Bullmore. Imaging structural co-variance between human brain regions. *Nat. Rev. Neurosci.*, 14:322–336, 2013.
- [56] A. C. Evans. Networks of anatomical covariance. *NeuroImage*, 80:489–504, 2013.
- [57] J. Seidlitz, F. Váša, M. Shinn, R. Romero-Garcia, K. J. Whitaker, P. E. Vértes, K. Wagstyl, P. Kirkpatrick Reardon, L. Clasen, S. Liu, A. Messinger, D. A. Leopold, P. Fonagy, R. J. Dolan, P. B. Jones, I. M. Goodyer, the NSPN Consortium, A. Raznahan, and E. T. Bullmore. Morphometric similarity networks detect microscale cortical organization and predict inter-individual cognitive variation. *Neuron*, 97:231–247, 2018.
- [58] J. Y. Hansen, G. Shafiei, R. D. Markello, K. Smart, S. M. L. Cox, M. Nørgaard, V. Beliveau, Y. Wu, J.-D. Gallezot, É. Aumont, S. Servaes, S. G. Scala, J. M. DuBois, G. Wainstein, G. Bezgin, T. Funck, T. W. Schmitz, R. N. Spreng, M. Galovic, M. J. Koepp, J. S. Duncan, J. P. Coles, T. D. Fryer, F. I. Aigbirhio, C. J. McGinnity, A. Hammers, J.-P. Soucy, S. Baillet, S. Guimond, J. Hietala, M.-A. Bedard, M. Leyton, E. Kobayashi, P. Rosa-Neto, M. Ganz, G. M. Knudsen, N. Palomero-Gallagher, J. M. Shine, R. E. Carson, L. Tuominen, A. Dagher, and B. Misic. Mapping neurotransmitter systems to the structural and functional organization of the human neocortex. *Nat. Neurosci.*, 25:1569–1581, 2022.
- [59] S. Horvath and J. Dong. Geometric interpretation of gene coexpression network analysis. *PLoS Comput. Biol.*, 4:e1000117, 2008.
- [60] P. Langfelder and S. Horvath. WGCNA: An R package for weighted correlation network analysis. *BMC Bioinformatics*, 9:559, 2008.
- [61] B. H. Junker and F. Schreiber, editors. *Analysis of Biological Networks*. John Wiley & Sons, Inc., Hoboken, NJ, 2008.
- [62] M. Vidal, M. E. Cusick, and A.-L. Barabási. Interactome networks and human disease. *Cell*, 144:986–998, 2011.
- [63] C. Gaiteri, Y. Ding, B. French, G. C. Tseng, and E. Sibille. Beyond modules and hubs: The potential of gene coexpression networks for investigating molecular mechanisms of complex brain disorders. *Genes Brain Behav.*, 13:13–24, 2014.
- [64] G. Fiscon, F. Conte, L. Farina, and P. Paci. Network-based approaches to explore complex biological systems towards network medicine. *Genes*, 9:437, 2018.
- [65] S. van Dam, U. Vösa, A. van der Graaf, L. Franke, and J. P. de Magalhães. Gene co-expression analysis for functional classification and gene–disease predictions. *Brief. Bioinfo.*, 19:575–592, 2018.
- [66] M. Mircea, M. Hochane, X. Fan, S. M. Chuva de Sousa Lopes, D. Garlaschelli, and S. Semrau. Phiclust: A clusterability measure for single-cell transcriptomics reveals phenotypic subpopulations. *Genome Biol.*, 23:18, 2022.
- [67] K. S. Parker, J. D. Wilson, J. Marschall, P. J. Mucha, and J. P. Henderson. Network analysis reveals sex- and antibiotic resistance-associated antivirulence targets in clinical uropathogens. *ACS Infectious Diseases*, 1:523–532, 2015.
- [68] Z. Zou, R. F. Potter, W. H. McCoy 4th, J. A. Wildenthal, G. L. Katumba, P. J. Mucha, G. Dantas, and J. P. Henderson. *E. coli* catheter-associated urinary tract infections are associated with distinctive virulence and biofilm gene determinants. *JCI Insight*, 8:e161461, 2023.

- [69] W.-C. Chou, A.-L. Cheng, M. Brotto, and C.-Y. Chuang. Visual gene-network analysis reveals the cancer gene co-expression in human endometrial cancer. *BMC Genomics*, 15:300, 2014.
- [70] R. Dobrin, J. Zhu, C. Molony, C. Argman, M. L. Parrish, S. Carlson, M. F. Allan, D. Pomp, and E. E. Schadt. Multi-tissue coexpression networks reveal unexpected subnetworks associated with disease. *Genome Biol.*, 10:R55, 2009.
- [71] Y. Xiang, J. Zhang, and K. Huang. Mining the tissue-tissue gene co-expression network for tumor microenvironment study and biomarker prediction. *BMC Genomics*, 14:S4, 2013.
- [72] L. J. A. Kogelman, J. Fu, L. Franke, J. W. Greve, M. Hofker, S. S. Rensen, and H. N. Kadarmideen. Intertissue gene co-expression networks between metabolically healthy and unhealthy obese individuals. *PLoS ONE*, 11:e0167519, 2016.
- [73] N. J. Hudson, A. Reverter, and B. P. Dalrymple. A differential wiring analysis of expression data correctly identifies the gene containing the causal mutation. *PLoS Comput. Biol.*, 5:e1000382, 2009.
- [74] R. Steuer. On the analysis and interpretation of correlations in metabolomic data. *Brief. Bioinfo.*, 7:151–158, 2006.
- [75] E. K. Silverman, H. H. H. W. Schmidt, E. Anastasiadou, L. Altucci, M. Angelini, L. Badimon, J.-L. Balligand, G. Benincasa, G. Capasso, F. Conte, A. Di Costanzo, L. Farina, G. Fiscon, L. Gatto, M. Gentili, J. Loscalzo, C. Marchese, C. Napoli, P. Paci, M. Petti, J. Quackenbush, P. Tieri, D. Viggiano, G. Vilahur, K. Glass, and J. Baumbach. Molecular networks in Network Medicine: Development and applications. *Wiley Interdisciplinary Reviews: Syst. Biol. Med.*, 12:e1489, 2020.
- [76] D. Camacho, A. de la Fuente, and P. Mendes. The origin of correlations in metabolomics data. *Metabolomics*, 1:53–63, 2005.
- [77] J. I. Robinson, W. H. Weir, J. R. Crowley, T. Hink, K. A. Reske, J. H. Kwon, C.-A. D. Burnham, E. R. Dubberke, P. J. Mucha, and J. P. Henderson. Metabolomic networks connect host-microbiome processes to human *Clostridioides difficile* infections. *J. Clin. Invest.*, 129:3792–3806, 2019.
- [78] H. Hirano and K. Takemoto. Difficulty in inferring microbial community structure based on co-occurrence network approaches. *BMC Bioinformatics*, 20:329, 2019.
- [79] M. Goberna and M. Verdú. Cautionary notes on the use of co-occurrence networks in soil ecology. *Soil Biol. Biochem.*, 166:108534, 2022.
- [80] J. M. Diamond. Assembly of species communities. In M. L. Cody and J. M. Diamond, editors, *Ecology and Evolution of Communities*, pages 342–444. Harvard University Press, Cambridge, MA, 1975.
- [81] J. X. Hu, C. E. Thomas, and S. Brunak. Network biology concepts in complex disease comorbidities. *Nat. Rev. Genet.*, 17:615–629, 2016.
- [82] C. A. Hidalgo, N. Blumm, A.-L. Barabási, and N. A. Christakis. A dynamic network approach for the study of human phenotypes. *PLoS Comput. Biol.*, 5:e1000353, 2009.
- [83] K.-I. Goh, M. E. Cusick, D. Valle, B. Childs, M. Vidal, and A.-L. Barabási. The human disease network. *Proc. Natl. Acad. Sci. USA*, 104:8685–8690, 2007.
- [84] A. Rzhetsky, D. Wajngurt, N. Park, and T. Zheng. Probing genetic overlap among complex human phenotypes. *Proc. Natl. Acad. Sci. USA*, 104:11694–11699, 2007.
- [85] D.-S. Lee, J. Park, K. A. Kay, N. A. Christakis, Z. N. Oltvai, and A.-L. Barabási. The implications of human metabolic network topology for disease comorbidity. *Proc. Natl. Acad. Sci. USA*, 105:9880–9885, 2008.
- [86] X. Zhou, J. Menche, A.-L. Barabási, and A. Sharma. Human symptoms–disease network. *Nat. Commun.*, 5:4212, 2014.
- [87] R. N. Mantegna and H. E. Stanley. *An Introduction to Econophysics*. Cambridge University Press, Cambridge, UK, 1999.

- [88] L. Laloux, P. Cizeau, J.-P. Bouchaud, and M. Potters. Noise dressing of financial correlation matrices. *Phys. Rev. Lett.*, 83:1467–1470, 1999.
- [89] V. Plerou, P. Gopikrishnan, B. Rosenow, L. A. Nunes Amaral, and H. E. Stanley. Universal and nonuniversal properties of cross correlations in financial time series. *Phys. Rev. Lett.*, 83:1471–1474, 1999.
- [90] M. MacMahon and D. Garlaschelli. Community detection for correlation matrices. *Phys. Rev. X*, 5:021006, 2015.
- [91] Almog, A. and Besamusca, F. and MacMahon, M. and Garlaschelli, D. Mesoscopic community structure of financial markets revealed by price and sign fluctuations. *PLoS ONE*, 10:e0133679, 2015.
- [92] S. M. Zema, G. Fagiolo, T. Squartini, and D. Garlaschelli. Mesoscopic structure of the stock market and portfolio optimization. *Preprint arXiv:2112.06544*, 2021.
- [93] I. Anagnostou, T. Squartini, D. Kandhai, and D. Garlaschelli. Uncovering the mesoscale structure of the credit default swap market to improve portfolio risk modelling. *Quantitative Finance*, 21:1501–1518, 2021.
- [94] R. N. Mantegna. Hierarchical structure in financial markets. *Eur. Phys. J. B*, 11:193–197, 1999.
- [95] M. Tumminello, F. Lillo, J. Piilo, and R. N. Mantegna. Identification of clusters of investors from their real trading activity in a financial market. *New J. Phys.*, 14:013041, 2012.
- [96] S. Ranganathan, M. Kivelä, and J. Kanninen. Dynamics of investor spanning trees around dot-com bubble. *PLoS ONE*, 13:e0198807, 2018.
- [97] D. Kercher. Inconsistent correlation and momenta: A new approach to portfolio allocation. MS Thesis. Brigham Young University, 2023.
- [98] E. Yan and Y. Ding. Scholarly network similarities: How bibliographic coupling networks, citation networks, cocitation networks, topical networks, coauthorship networks, and coword networks relate to each other. *J. Amer. Soc. Info. Sci. Tech.*, 63:1313–1326, 2012.
- [99] J.-P. Qiu, K. Dong, and H.-Q. Yu. Comparative study on structure and correlation among author co-occurrence networks in bibliometrics. *Scientometrics*, 101:1345–1360, 2014.
- [100] M. E. J. Newman. Scientific collaboration networks. II. Shortest paths, weighted networks, and centrality. *Phys. Rev. E*, 64:016132, 2001.
- [101] C. Cattuto, A. Barrat, A. Baldassarri, G. Schehr, and V. Loreto. Collective dynamics of social annotation. *Proc. Natl. Acad. Sci. USA*, 106:10511–10515, 2009.
- [102] F. Luo, J. Z. Wang, and E. Promislow. Exploring local community structures in large networks. In *Proceedings of 2006 IEEE/WIC/ACM International Conference on Web Intelligence (WI'06)*, pages 233–239, 2006.
- [103] A. A. Tsonis and P. J. Roebber. The architecture of the climate network. *Physica A*, 333:497–504, 2004.
- [104] A. A. Tsonis, K. L. Swanson, and P. J. Roebber. What do networks have to do with climate? *Bull. Amer. Meteorol. Soc.*, 87:585–595, 2006.
- [105] J. F. Donges, Y. Zou, N. Marwan, and J. Kurths. The backbone of the climate network. *EPL*, 87:48007, 2009.
- [106] J. Fan, J. Meng, J. Ludescher, X. Chen, Y. Ashkenazy, J. Kurths, S. Havlin, and H. J. Schellnhuber. Statistical physics approaches to the complex Earth system. *Phys. Rep.*, 896:1–84, 2021.
- [107] J. Heitzig, J. F. Donges, Y. Zou, N. Marwan, and J. Kurths. Node-weighted measures for complex networks with spatially embedded, sampled, or differently sized nodes. *Eur. Phys. J. B*, 85:38, 2012.
- [108] S. Scarsoglio, F. Laio, and L. Ridolfi. Climate dynamics: A network-based approach for the analysis of global precipitation. *PLoS ONE*, 8:e71129, 2013.
- [109] M. van der Mheen, H. A. Dijkstra, A. Gozolchiani, M. den Toom, Q. Feng, J. Kurths, and E. Hernandez-Garcia. Interaction network based early warning indicators for the Atlantic MOC collapse. *Geophys. Res. Lett.*, 40:2714–2719, 2013.

- [110] P. J. Bickel and E. Levina. Covariance regularization by thresholding. *Ann. Stat.*, 36:2577–2604, 2008.
- [111] M. Pourahmadi. Covariance estimation: The GLM and regularization perspectives. *Statist. Sci.*, 26:369–387, 2011.
- [112] J. Fan, Y. Liao, and H. Liu. An overview of the estimation of large covariance and precision matrices. *Econometrics J.*, 19:C1–C32, 2016.
- [113] J. Whittaker. *Graphical Models in Applied Multivariate Statistics*. John Wiley & Sons, Chichester, UK, 1990.
- [114] S. L. Lauritzen. *Graphical Models*. Clarendon Press, Oxford, UK, 1996.
- [115] A. P. Dempster. Covariance selection. *Biometrics*, 28:157–175, 1972.
- [116] O. Ledoit and M. Wolf. The power of (non-)linear shrinking: A review and guide to covariance matrix estimation. *J. Financial Econometrics*, 20:187–218, 2022.
- [117] O. Ledoit and M. Wolf. Improved estimation of the covariance matrix of stock returns with an application to portfolio selection. *J. Empirical Finance*, 10:603–621, 2003.
- [118] O. Ledoit and M. Wolf. A well-conditioned estimator for large-dimensional covariance matrices. *J. Multivar. Anal.*, 88:365–411, 2004.
- [119] Y. Chen, A. Wiesel, Y. C. Eldar, and A. O. Hero. Shrinkage algorithms for MMSE covariance estimation. *IEEE Trans. Signal Proc.*, 58:5016–5029, 2010.
- [120] R. B. Holmes. On random correlation matrices. *SIAM J. Matrix Anal. Appl.*, 12:239–272, 1991.
- [121] J. A. Tropp. Simplicial faces of the set of correlation matrices. *Discrete Comput. Geom.*, 60:512–529, 2018.
- [122] Y. Thanwerdas and X. Pennec. Geodesics and curvature of the quotient-affine metrics on full-rank correlation matrices. *Lect. Notes Comput. Sci.*, 12829:93–102, 2021.
- [123] M. Rubinov and O. Sporns. Weight-conserving characterization of complex functional brain networks. *NeuroImage*, 56:2068–2079, 2011.
- [124] K. A. Garrison, D. Scheinost, E. S. Finn, X. Shen, and R. T. Constable. The (in)stability of functional brain network measures across thresholds. *NeuroImage*, 118:651–661, 2015.
- [125] F. De Vico Fallani, V. Latora, and M. Chavez. A topological criterion for filtering information in complex brain networks. *PLoS Comput. Biol.*, 13:e1005305, 2017.
- [126] M. W. Cole, S. Pathak, and W. Schneider. Identifying the brain’s most globally connected regions. *NeuroImage*, 49:3132–3148, 2010.
- [127] D. Scheinost, J. Benjamin, C. M. Lacadie, B. Vohr, K. C. Schneider, L. R. Ment, X. Papademetris, and R. T. Constable. The intrinsic connectivity distribution: A novel contrast measure reflecting voxel level functional connectivity. *NeuroImage*, 62:1510–1519, 2012.
- [128] L. Peel, T. P. Peixoto, and M. De Domenico. Statistical inference links data and theory in network science. *Nat. Commun.*, 13:6794, 2022.
- [129] M. P. van den Heuvel, S. C. de Lange, A. Zalesky, C. Seguin, B. T. T. Yeo, and R. Schmidt. Proportional thresholding in resting-state fMRI functional connectivity networks and consequences for patient-control connectome studies: Issues and recommendations. *NeuroImage*, 152:437–449, 2017.
- [130] S. Achard and E. Bullmore. Efficiency and cost of economical brain functional networks. *PLoS Comput. Biol.*, 3:e17, 2007.
- [131] M. P. van den Heuvel, C. J. Stam, M. Boersma, and H. E. Hulshoff Pol. Small-world and scale-free organization of voxel-based resting-state functional connectivity in the human brain. *NeuroImage*, 43:528–539, 2008.
- [132] J. Wang, L. Wang, Y. Zang, H. Yang, H. Tang, Q. Gong, Z. Chen, C. Zhu, and Y. He. Parcellation-dependent small-world brain functional networks: A resting-state fMRI study. *Human Brain Mapping*, 30:1511–1523, 2009.

- [133] B. C. M. van Wijk, C. J. Stam, and A. Daffertshofer. Comparing brain networks of different size and connectivity density using graph theory. *PLoS ONE*, 5:e13701, 2010.
- [134] A. F. Alexander-Bloch, N. Gogtay, D. Meunier, R. Birn, L. Clasen, F. Lalonde, R. Lenroot, J. Giedd, and E. T. Bullmore. Disrupted modularity and local connectivity of brain functional networks in childhood-onset schizophrenia. *Front. Syst. Neurosci.*, 4:147, 2010.
- [135] E. Langford, N. Schwertman, and M. Owens. Is the property of being positively correlated transitive? *Am. Stat.*, 55:322–325, 2001.
- [136] J. Gillis and P. Pavlidis. The role of indirect connections in gene networks in predicting function. *Bioinformatics*, 27:1860–1866, 2011.
- [137] A. Zalesky, A. Fornito, and E. Bullmore. On the use of correlation as a measure of network connectivity. *NeuroImage*, 60:2096–2106, 2012.
- [138] M. Barthélemy. Spatial networks. *Phys. Rep.*, 499:1–101, 2011.
- [139] M. Barthelemy. *Morphogenesis of Spatial Networks*. Springer, Cham, Switzerland, 2018.
- [140] N. Langer, A. Pedroni, and L. Jäncke. The problem of thresholding in small-world network analysis. *PLoS ONE*, 8:e53199, 2013.
- [141] M.-E. Lynall, D. S. Bassett, R. Kerwin, P. J. McKenna, M. Kitzbichler, U. Muller, and E. Bullmore. Functional connectivity and brain networks in schizophrenia. *J. Neurosci.*, 30:9477–9487, 2010.
- [142] C. E. Ginestet, T. E. Nichols, E. T. Bullmore, and A. Simmons. Brain network analysis: Separating cost from topology using cost-integration. *PLoS ONE*, 6:e21570, 2011.
- [143] D. S. Bassett, B. G. Nelson, B. A. Mueller, J. Camchong, and K. O. Lim. Altered resting state complexity in schizophrenia. *NeuroImage*, 59:2196–2207, 2012.
- [144] S. M. H. Hosseini, F. Hoefft, and S. R. Kesler. GAT: A graph-theoretical analysis toolbox for analyzing between-group differences in large-scale structural and functional brain networks. *PLoS ONE*, 7:e40709, 2012.
- [145] V. Latora and M. Marchiori. Efficient behavior of small-world networks. *Phys. Rev. Lett.*, 87:198701, 2001.
- [146] D. S. Bassett, A. Meyer-Lindenberg, S. Achard, T. Duke, and E. Bullmore. Adaptive reconfiguration of fractal small-world human brain functional networks. *Proc. Natl. Acad. Sci. USA*, 103:19518–19523, 2006.
- [147] N. Vandewalle, F. Brisbois, and X. Tordoir. Non-random topology of stock markets. *Quant. Finance*, 1:372–374, 2001.
- [148] J.-P. Onnela, A. Chakraborti, K. Kaski, and J. Kertész. Dynamic asset trees and portfolio analysis. *Eur. Phys. J. B*, 30:285–288, 2002.
- [149] M. Tumminello, T. Aste, T. Di Matteo, and R. N. Mantegna. A tool for filtering information in complex systems. *Proc. Natl. Acad. Sci. USA*, 102:10421–10426, 2005.
- [150] M. Á Serrano, M. Boguñá, and A. Vespignani. Extracting the multiscale backbone of complex weighted networks. *Proc. Natl. Acad. Sci. USA*, 106:6483–6488, 2009.
- [151] S. Horvath. *Weighted Network Analysis*. Springer, New York, NY, 2011.
- [152] D. L. Donoho and I. M. Johnstone. Ideal spatial adaptation by wavelet shrinkage. *Biometrika*, 81:425–455, 1994.
- [153] N. El Karoui. Operator norm consistent estimation of large-dimensional sparse covariance matrices. *Ann. Stat.*, 36:2717–2756, 2008.
- [154] A. J. Rothman, E. Levina, and J. Zhu. Generalized thresholding of large covariance matrices. *J. Am. Stat. Assoc.*, 104:177–186, 2009.
- [155] R. Tibshirani. Regression shrinkage and selection via the lasso. *J. R. Statist. Soc. B*, 58:267–288, 1996.

- [156] T. Cai and W. Liu. Adaptive thresholding for sparse covariance matrix estimation. *J. Am. Stat. Assoc.*, 106:672–684, 2011.
- [157] K. R. A. Van Dijk, T. Hedden, A. Venkataraman, K. C. Evans, S. W. Lazar, and R. L. Buckner. Intrinsic functional connectivity as a tool for human connectomics: Theory, properties, and optimization. *J. Neurophysiol.*, 103:297–321, 2010.
- [158] J. Tang, Y. Chang, C. Aggarwal, and H. Liu. A survey of signed network mining in social media. *ACM Comput. Surv.*, 49:42, 2016.
- [159] L. Zhan, L. M. Jenkins, O. E. Wolfson, J. J. GadElkarim, K. Nocito, P. M. Thompson, O. A. Ajilore, M. K. Chung, and A. D. Leow. The significance of negative correlations in brain connectivity. *J. Comparative Neurol.*, 525:3251–3265, 2017.
- [160] S. Gómez, P. Jensen, and A. Arenas. Analysis of community structure in networks of correlated data. *Phys. Rev. E*, 80:016114, 2009.
- [161] C. Aicher, A. Z. Jacobs, and A. Clauset. Learning latent block structure in weighted networks. *J. Comp. Netw.*, 3:221–248, 2015.
- [162] T. P. Peixoto. Nonparametric weighted stochastic block models. *Phys. Rev. E*, 97:012306, 2018.
- [163] A. de la Fuente, N. Bing, I. Hoeschele, and P. Mendes. Discovery of meaningful associations in genomic data using partial correlation coefficients. *Bioinformatics*, 20:3565–3574, 2004.
- [164] R. Salvador, J. Suckling, M. R. Coleman, J. D. Pickard, D. Menon, and E. Bullmore. Neurophysiological architecture of functional magnetic resonance images of human brain. *Cereb. Cortex*, 15:1332–1342, 2005.
- [165] G. Marrelec, A. Krainik, H. Duffau, M. Péligrini-Issac, S. Lehericy, J. Doyon, and H. Benali. Partial correlation for functional brain interactivity investigation in functional MRI. *NeuroImage*, 32:228–237, 2006.
- [166] M. Goldstein and A. F. M. Smith. Ridge-type estimators for regression analysis. *J. R. Statist. Soc. Ser. B*, 36:284–291, 1974.
- [167] A. Hero and B. Rajaratnam. Hub discovery in partial correlation graphs. *IEEE Trans. Info. Th.*, 58:6064–6078, 2012.
- [168] R. Artner, P. P. Wellingerhof, G. Lafit, T. Loossens, W. Vanpaemel, and F. Tuerlinckx. The shape of partial correlation matrices. *Commun. Stat.*, 51:4133–4150, 2022.
- [169] T. Aste and T. Di Matteo. Dynamical networks from correlations. *Physica A*, 370:156–161, 2006.
- [170] D. R. Williams. Learning to live with sampling variability: Expected replicability in partial correlation networks. *Psychol. Methods*, 27:606–621, 2022.
- [171] T. Millington and M. Niranjana. Partial correlation financial networks. *Appl. Netw. Sci.*, 5:11, 2020.
- [172] N. Meinshausen and P. Bühlmann. High-dimensional graphs and variable selection with the Lasso. *Ann. Stat.*, 34:1436–1462, 2006.
- [173] M. Yuan and Y. Lin. Model selection and estimation in the Gaussian graphical model. *Biometrika*, 94:19–35, 2007.
- [174] O. Banerjee, L. El Ghaoui, and A. d’Aspremont. Model selection through sparse maximum likelihood estimation for multivariate Gaussian or binary data. *J. Machine Learning Res.*, 9:485–516, 2008.
- [175] J. Friedman, T. Hastie, and R. Tibshirani. Sparse inverse covariance estimation with the graphical lasso. *Biostatistics*, 9:432–441, 2008.
- [176] J. Fan, Y. Feng, and Y. Wu. Network exploration via the adaptive LASSO and SCAD penalties. *Ann. Appl. Stat.*, 3:521–541, 2009.
- [177] R. Foygel and M. Drton. Extended Bayesian information criteria for Gaussian graphical models. *Advances in Neural Information Processing Systems 23*, 23:604–612, 2010.

- [178] T. Hastie, R. Tibshirani, and M. Wainwright. *Statistical Learning with Sparsity: The Lasso and Generalizations*. CRC Press, Boca Raton, FL, 2015.
- [179] J. Schäfer and K. Strimmer. An empirical Bayes approach to inferring large-scale gene association networks. *Bioinformatics*, 21:754–764, 2005.
- [180] H. Li and J. Gui. Gradient directed regularization for sparse Gaussian concentration graphs, with applications to inference of genetic networks. *Biostatistics*, 7:302–317, 2006.
- [181] A. d’Aspremont, O. Banerjee, and L. El Ghaoui. First-order methods for sparse covariance selection. *SIAM J. Matrix Anal. Appl.*, 30:56–66, 2008.
- [182] J. Z. Huang, N. Liu, M. Pourahmadi, and L. Liu. Covariance matrix selection and estimation via penalised normal likelihood. *Biometrika*, 93:85–98, 2006.
- [183] J. Bien and R. J. Tibshirani. Sparse estimation of a covariance matrix. *Biometrika*, 98:807–820, 2011.
- [184] H. Wang. Coordinate descent algorithm for covariance graphical lasso. *Stat. Comput.*, 24:521–529, 2014.
- [185] H. Wang. Scaling it up: Stochastic search structure learning in graphical models. *Bayesian Analysis*, 10:351–377, 2015.
- [186] S. Kojaku and N. Masuda. Constructing networks by filtering correlation matrices: A null model approach. *Proc. R Soc. A*, 475:20190578, 2019.
- [187] N. Masuda and R. Lambiotte. *A Guide to Temporal Networks*. World Scientific, Singapore, second edition, 2020.
- [188] P. Holme and J. Saramäki. Temporal networks. *Phys. Rep.*, 519:97–125, 2012.
- [189] P. Holme. Modern temporal network theory: A colloquium. *Eur. Phys. J. B*, 88:234, 2015.
- [190] M. Bazzi, M. A. Porter, S. Williams, M. McDonald, D. J. Fenn, and S. D. Howison. Community detection in temporal multilayer networks, with an application to correlation networks. *Multiscale Model. Simul.*, 1:1–41, 2016.
- [191] R. Hindriks, M. H. Adhikari, Y. Murayama, M. Ganzetti, D. Mantini, N. K. Logothetis, and G. Deco. Can sliding-window correlations reveal dynamic functional connectivity in resting-state fMRI? *NeuroImage*, 127:242–256, 2016.
- [192] Z. Adams, R. Füss, and T. Glück. Are correlations constant? Empirical and theoretical results on popular correlation models in finance. *J. Banking Finance*, 84:9–24, 2017.
- [193] M. A. Lindquist, Y. Xu, M. B. Nebel, and B. S. Caffo. Evaluating dynamic bivariate correlations in resting-state fMRI: A comparison study and a new approach. *NeuroImage*, 101:531–546, 2014.
- [194] J.-P. Onnela, A. Chakraborti, K. Kaski, J. Kertész, and A. Kanto. Dynamics of market correlations: Taxonomy and portfolio analysis. *Phys. Rev. E*, 68:056110, 2003.
- [195] J.-P. Onnela, K. Kaski, and J. Kertész. Clustering and information in correlation based financial networks. *Eur. Phys. J. B*, 38:353–362, 2004.
- [196] R. M. Hutchison, T. Womelsdorf, E. A. Allen, P. A. Bandettini, V. D. Calhoun, M. Corbetta, S. Della Penna, J. H. Duyn, G. H. Glover, J. Gonzalez-Castillo, D. A. Handwerker, S. Keilholz, V. Kiviniemi, D. A. Leopold, F. de Pasquale, O. Sporns, M. Walter, and C. Chang. Dynamic functional connectivity: Promise, issues, and interpretations. *NeuroImage*, 80:360–378, 2013.
- [197] V. D. Calhoun, R. Miller, G. Pearlson, and T. Adali. The chronnectome: Time-varying connectivity networks as the next frontier in fMRI data discovery. *Neuron*, 84:262–274, 2014.
- [198] M. Filippi, E. G. Spinelli, C. Cividini, and F. Agosta. Resting state dynamic functional connectivity in neurodegenerative conditions: A review of magnetic resonance imaging findings. *Front. Neurosci.*, 13:657, 2019.

- [199] D. J. Lurie, D. Kessler, D. S. Bassett, R. F. Betzel, M. Breakspear, S. Kheilholz, A. Kucyi, R. Liégeois, M. A. Lindquist, A. R. McIntosh, R. A. Poldrack, J. M. Shine, W. H. Thompson, N. Z. Bielczyk, L. Douw, D. Kraft, R. L. Miller, M. Muthuraman, L. Pasquini, A. Razi, D. Vidaurre, H. Xie, and V. D. Calhoun. Questions and controversies in the study of time-varying functional connectivity in resting fMRI. *Netw. Neurosci.*, 4:30–69, 2020.
- [200] D. S. Bassett, N. F. Wymbs, M. A. Porter, P. J. Mucha, J. M. Carlson, and S. T. Grafton. Dynamic reconfiguration of human brain networks during learning. *Proc. Natl. Acad. Sci. USA*, 108:7641–7646, 2011.
- [201] D. S. Bassett, N. F. Wymbs, M. P. Rombach, M. A. Porter, P. J. Mucha, and S. T. Grafton. Task-based core-periphery organization of human brain dynamics. *PLoS Comput. Biol.*, 9:e1003171, 2013.
- [202] U. Braun, A. Schäfer, H. Walter, S. Erk, N. Romanczuk-Seiferth, L. Haddad, J. I. Schweiger, O. Grimm, A. Heinz, H. Tost, A. Meyer-Lindenberg, and D. S. Bassett. Dynamic reconfiguration of frontal brain networks during executive cognition in humans. *Proc. Natl. Acad. Sci. USA*, 112:11678–11683, 2015.
- [203] J. Nakajima and M. West. Bayesian analysis of latent threshold dynamic models. *J. Busi. Econ. Stat.*, 31:151–164, 2013.
- [204] J. Nakajima and M. West. Dynamic network signal processing using latent threshold models. *Digital Signal Proc.*, 47:5–16, 2015.
- [205] D. Hallac, Y. Park, S. Boyd, and J. Leskovec. Network inference via the time-varying graphical lasso. In *Proceedings of the 23th ACM SIGKDD International Conference on Knowledge Discovery and Data Mining*, pages 205–213, 2017.
- [206] D. J. Watts and S. H. Strogatz. Collective dynamics of ‘small-world’ networks. *Nature*, 393:440–442, 1998.
- [207] B. K. Fosdick, D. B. Larremore, J. Nishimura, and J. Ugander. Configuring random graph models with fixed degree sequences. *SIAM Review*, 60:315–355, 2018.
- [208] F. Váša and B. Mišić. Null models in network neuroscience. *Nat. Rev. Neurosci.*, 23:493–504, 2022.
- [209] R. Milo, S. Shen-Orr, S. Itzkovitz, N. Kashtan, D. Chklovskii, and U. Alon. Network motifs: simple building blocks of complex networks. *Science*, 298:824–827, 2002.
- [210] S. Fortunato. Community detection in graphs. *Phys. Rep.*, 486:75–174, 2010.
- [211] V. Colizza, M. A. Serrano A. Flammini, and A. Vespignani. Detecting rich-club ordering in complex networks. *Nat. Phys.*, 2:110–115, 2006.
- [212] S. Kojaku and N. Masuda. Core-periphery structure requires something else in the network. *New J. Phys.*, 20:043012, 2018.
- [213] P. Expert, T. S. Evans, V. D. Blondel, and R. Lambiotte. Uncovering space-independent communities in spatial networks. *Proc. Natl. Acad. Sci. USA*, 108:7663–7668, 2011.
- [214] T. Squartini, R. Mastrandrea, and D. Garlaschelli. Unbiased sampling of network ensembles. *New J. Phys.*, 17:023052, 2015.
- [215] T. Squartini and D. Garlaschelli. *Maximum-Entropy Networks*. Springer, Cham, Switzerland, 2017.
- [216] E. Valdano and A. Arenas. Exact rank reduction of network models. *Phys. Rev. X*, 9:031050, 2019.
- [217] M. E. J. Newman. *Networks*. Oxford University Press, Oxford, UK, second edition, 2018.
- [218] N. Masuda, S. Kojaku, and Y. Sano. Configuration model for correlation matrices preserving the node strength. *Phys. Rev. E*, 98:012312, 2018.
- [219] W. Böhm and K. Hornik. Generating random correlation matrices by the simple rejection method: Why it does not work. *Stat. Prob. Lett.*, 87:27–30, 2014.
- [220] J. Theiler, S. Eubank, A. Longtin, B. Galdrikian, and J. D. Farmer. Testing for nonlinearity in time series: The method of surrogate data. *Physica D*, 58:77–94, 1992.

- [221] T. Schreiber and A. Schmitz. Surrogate time series. *Physica D*, 142:346–382, 2000.
- [222] M. Shinn, A. Hu, L. Turner, S. Noble, K. H. Preller, J. L. Ji, F. Moujaes, S. Achard, D. Scheinost, R. T. Constable, J. H. Krystal, F. X. Vollenweider, D. Lee, A. Anticevic, E. T. Bullmore, and J. D. Murray. Functional brain networks reflect spatial and temporal autocorrelation. *Nat. Neurosci.*, 26:867–878, 2023.
- [223] M. Hirschberger, Y. Qi, and R. E. Steuer. Randomly generating portfolio-selection covariance matrices with specified distributional characteristics. *Eur. J. Oper. Res.*, 177:1610–1625, 2007.
- [224] A. Fornito, A. Zalesky, and M. Breakspear. Graph analysis of the human connectome: Promise, progress, and pitfalls. *NeuroImage*, 80:426–444, 2013.
- [225] A. L. Barabási. *Network Science*. Cambridge University Press, Cambridge, UK, 2016.
- [226] A. Barrat, M. Barthélemy, R. Pastor-Satorras, and A. Vespignani. The architecture of complex weighted networks. *Proc. Natl. Acad. Sci. USA*, 101:3747–3752, 2004.
- [227] V. M. Eguíluz, D. R. Chialvo, G. A. Cecchi, M. Baliki, and A. V. Apkarian. Scale-free brain functional networks. *Phys. Rev. Lett.*, 94:018102, 2005.
- [228] B. Zhang and S. Horvath. A general framework for weighted gene co-expression network analysis. *Stat. Appl. Genet. Mol. Biol.*, 4:17, 2005.
- [229] D. S. Bassett, E. Bullmore, B. A. Verchinski, V. S. Mattay, D. R. Weinberger, and A. Meyer-Lindenberg. Hierarchical organization of human cortical networks in health and schizophrenia. *J. Neurosci.*, 28:9239–9248, 2008.
- [230] M. A. Porter, J.-P. Onnela, and P. J. Mucha. Communities in networks. *Notices of the AMS*, 56:1082–1097, 1164–1166, 2009.
- [231] A. Almog, M. R. Buijink, O. Roethler, S. Michel, J. H. Meijer, J. H. T. Rohling, and D. Garlaschelli. Uncovering functional signature in neural systems via random matrix theory. *PLoS Comput. Biol.*, 15:e1006934, 2019.
- [232] J. Saramäki, M. Kivelä, J.-P. Onnela, K. Kaski, and J. Kertész. Generalizations of the clustering coefficient to weighted complex networks. *Phys. Rev. E*, 75:027105, 2007.
- [233] Y. Wang, E. Ghumare, R. Vandenberghe, and P. Dupont. Comparison of different generalizations of clustering coefficient and local efficiency for weighted undirected graphs. *Neural Comput.*, 29:313–331, 2017.
- [234] N. Masuda, M. Sakaki, T. Ezaki, and T. Watanabe. Clustering coefficients for correlation networks. *Front. Neuroinfo.*, 12:7, 2018.
- [235] phiclust: A clusterability measure for scRNA-seq data. <https://github.com/semraulab/phiclust>. Accessed: 13 November 2023.
- [236] Mircea, M. and Hochane, M. and Fan, X. and Chuva de Sousa Lopes, S. M. and Garlaschelli, D. and Semrau, S. Phiclust: A clusterability measure for single-cell transcriptomics reveals phenotypic subpopulations. <https://zenodo.org/record/5785793#.Ybs5wn3MK3I>. Accessed: 13 November 2023.
- [237] M. Rubinov and O. Sporns. Complex network measures of brain connectivity: Uses and interpretations. *NeuroImage*, 52:1059–1069, 2010.
- [238] T. P. Peixoto. The graph-tool python library. http://figshare.com/articles/graph_tool/1164194. Accessed: 14 November 2023.
- [239] M. O. Kuusmin and M. J. Sillanpää. Estimation of covariance and precision matrix, network structure, and a view toward systems biology. *WIREs Comput. Stat.*, 9:e1415, 2017.
- [240] S. Epskamp, A. O. J. Cramer, L. J. Waldorp, V. D. Schmittmann, and D. Borsboom. qgraph: Network visualizations of relationships in psychometric data. *J. Stat. Software*, 48:1–18, 2012.
- [241] R. R. Gabriel. Estimating a psychometric network with qgraph. <https://reisrgabriel.com/blog/2021-08-10-psych-network/>. Accessed: 24 August 2023.

- [242] F. Pedregosa, G. Varoquaux, A. Gramfort, V. Michel, B. Thirion, O. Grisel, M. Blondel, P. Prettenhofer, R. Weiss, V. Dubourg, J. Vanderplas, A. Passos, D. Cournapeau, M. Brucher, M. Perrot, and É. Duchesnay. Scikit-learn: Machine learning in Python. *J. Mach. Learn. Res.*, 12:2825–2830, 2011.
- [243] Scikit-learn package. <https://scikit-learn.org/stable/install.html>. Accessed: 18 May 2022.
- [244] Mel. Random matrix theory (rmt) filtering of financial time series for community detection. <http://www.mathworks.com/matlabcentral/fileexchange/49011>. Accessed: 13 November 2023.
- [245] M. W. Cole, T. Yarkoni, G. Repovs, A. Anticevic, and T. S. Braver. Global connectivity of prefrontal cortex predicts cognitive control and intelligence. *J. Neurosci.*, 32:8988–8999, 2012.
- [246] E. Santarnecchi, G. Galli, N. R. Polizzotto, A. Rossi, and S. Rossi. Efficiency of weak brain connections support general cognitive functioning. *Human Brain Mapping*, 35:4566–4582, 2014.
- [247] J.-G. Young, G. T. Cantwell, and M. E. J. Newman. Bayesian inference of network structure from unreliable data. *J. Compl. Netw.*, 8:cnaa046, 2020.
- [248] S. Boccaletti, G. Bianconi, R. Criado, C. I. del Genio, J. Gómez-Gardeñes, M. Romance, I. Sendiña Nadal, Z. Wang, and M. Zanin. The structure and dynamics of multilayer networks. *Phys. Rep.*, 544:1–122, 2014.
- [249] M. Kivelä, A. Arenas, M. Barthelemy, J. P. Gleeson, Y. Moreno, and M. A. Porter. Multilayer networks. *J. Comp. Netw.*, 2:203–271, 2014.
- [250] G. Bianconi. *Multilayer Networks*. Oxford University Press, Oxford, UK, 2018.
- [251] M. J. Brookes, P. K. Tewarie, B. A. E. Hunt, S. E. Robson, L. E. Gascoyne, E. B. Liddle, P. F. Liddle, and P. G. Morris. A multi-layer network approach to MEG connectivity analysis. *NeuroImage*, 132:425–438, 2016.
- [252] P. Tewarie, A. Hillebrand, B. W. van Dijk, C. J. Stam, G. C. O’Neill, P. Van Mieghem, J. M. Meier, M. W. Woolrich, P. G. Morris, and M. J. Brookes. Integrating cross-frequency and within band functional networks in resting-state MEG: A multi-layer network approach. *NeuroImage*, 142:324–336, 2016.
- [253] J. M. Buldú and M. A. Porter. Frequency-based brain networks: From a multiplex framework to a full multilayer description. *Netw. Neurosci.*, 2:418–441, 2017.
- [254] M. De Domenico, S. Sasai, and A. Arenas. Mapping multiplex hubs in human functional brain networks. *Front. Neurosci.*, 10:326, 2016.
- [255] M. De Domenico. Multilayer modeling and analysis of human brain networks. *GigaScience*, 6:gix004, 2017.
- [256] R. Dorantes-Gilardi, D. García-Cortés, E. Hernández-Lemus, and J. Espinal-Enríquez. Multilayer approach reveals organizational principles disrupted in breast cancer co-expression networks. *Appl. Netw. Sci.*, 5:47, 2020.
- [257] M. Russell, A. Aqil, M. Saitou, O. Gokcumen, and N. Masuda. Gene communities in co-expression networks across different tissues. *PLoS Comput. Biol.*, 00:in press, 2023.
- [258] N. Musmeci, V. Nicosia, T. Aste, T. Di Matteo, and V. Latora. The multiplex dependency structure of financial markets. *Complexity*, 2017:9586064, 2017.
- [259] P. J. Mucha, T. Richardson, K. Macon, M. A. Porter, and J.-P. Onnela. Community structure in time-dependent, multiscale, and multiplex networks. *Science*, 328:876–878, 2010.
- [260] D. Taylor, S. Shai, N. Stanley, and P. J. Mucha. Enhanced detectability of community structure in multilayer networks through layer aggregation. *Phys. Rev. Lett.*, 116:228301, 2016.
- [261] D. Taylor, R. S. Caceres, and P. J. Mucha. Super-resolution community detection for layer-aggregated multilayer networks. *Phys. Rev. X*, 7:031056, 2017.
- [262] M. Venkatesh, J. Jaja, and L. Pessoa. Comparing functional connectivity matrices: A geometry-aware approach applied to participant identification. *NeuroImage*, 207:116398, 2020.
- [263] K. You and H.-J. Park. Re-visiting Riemannian geometry of symmetric positive definite matrices for the analysis of functional connectivity. *NeuroImage*, 225:117464, 2021.

- [264] K. Abbas, M. Liu, M. Venkatesh, E. Amico, A. D. Kaplan, M. Ventresca, L. Pessoa, J. Harezlak, and J. Goñi. Geodesic distance on optimally regularized functional connectomes uncovers individual fingerprints. *Brain Conn.*, 11:333–348, 2021.
- [265] X. Pennec, P. Fillard, and N. Ayache. A Riemannian framework for tensor computing. *Int. J. Comput. Vis.*, 66:41–66, 2006.
- [266] M. Rahim, B. Thirion, and G. Varoquaux. Population shrinkage of covariance (PoSCE) for better individual brain functional-connectivity estimation. *Med. Image Anal.*, 54:138–148, 2019.
- [267] L. Lovász. *Large Networks and Graph Limits*. American Mathematical Society, Providence, RI, 2012.
- [268] G. Bianconi and A.-L. Barabási. Bose-Einstein condensation in complex networks. *Phys. Rev. Lett.*, 86:5632–5635, 2001.
- [269] G. Bianconi and A.-L. Barabási. Competition and multiscaling in evolving networks. *Europhys. Lett.*, 54:436–442, 2001.
- [270] K.-I. Goh, B. Kahng, and D. Kim. Universal behavior of load distribution in scale-free networks. *Phys. Rev. Lett.*, 87:278701, 2001.
- [271] G. Caldarelli, A. Capocci, P. De Los Rios, and M. A. Muñoz. Scale-free networks from varying vertex intrinsic fitness. *Phys. Rev. Lett.*, 89:258702, 2002.
- [272] M. Boguna and R. Pastor-Satorras. Class of correlated random networks with hidden variables. *Phys. Rev. E*, 68:036112, 2003.
- [273] N. Masuda, H. Miwa, and N. Konno. Analysis of scale-free networks based on a threshold graph with intrinsic vertex weights. *Phys. Rev. E*, 70:036124, 2004.
- [274] N. Perra, B. Gonçalves, R. Pastor-Satorras, and A. Vespignani. Activity driven modeling of time varying networks. *Sci. Rep.*, 2:469, 2012.
- [275] N. Masuda, H. Miwa, and N. Konno. Geographical threshold graphs with small-world and scale-free properties. *Phys. Rev. E*, 71:036108, 2005.
- [276] N. Masuda and N. Konno. VIP-club phenomenon: Emergence of elites and masterminds in social networks. *Soc. Netw.*, 28:297–309, 2006.
- [277] G. T. Cantwell, Y. Liu, B. F. Maier, A. C. Schwarze, C. A. Serván, J. Snyder, and G. St-Onge. Thresholding normally distributed data creates complex networks. *Phys. Rev. E*, 101:062302, 2020.